UNIVERSITÀ DEGLI STUDI DELL'INSUBRIA

FACOLTÀ DI SCIENZE MATICHE FISICHE E NATURALI

Ph.D. SCHOOL OF BIOLOGICAL AND MEDICAL SCIENCES

UNIVERSITY OF INSUBRIA

Ph.D. course in Biotechnology, XXIII cycle

Functional characterization of the tumor antagonizing gene RNASET2

Ph.D. thesis of Paolo Bonetti

Tutor Prof. Roberto Taramelli

Table of contents

1. Summary

Several types of cancer including solid tumors and blood malignancies are associated with alterations in different regions of chromosome 6. In particular, the 6q region has been frequently found to be deleted in a wide range of solid tumors, including ovarian carcinoma. Therefore, this chromosomal region has been extensively investigated in order to identifying putative tumor suppressor genes. In specific, a minimal region of deletion for ovarian cancer has been defined in the peritelomeric 6q27 region, and our group has recently isolated from this region the RNASET2 gene, coding for a secreted ribonuclease belonging to the Rh/T2/S acid ribonuclease family.

The RNASET2 gene was found to be down-regulated at the transcriptional level in several primary ovarian tumors and ovarian cancer cell lines and its potential for tumor growth inhibition has been subsequently tested *in vivo* in a highly tumorigenic and metastatic Hey3Met2 ovarian cancer cell line.
To this aim, athymic mice were injected with Hey3Met2 cell clones stably transfected with expression vectors encoding wild-type or a catalytically inactive mutant RNASET2 protein. Strikingly, wild-type RNASET2-expressing cells formed smaller tumors in mice and gave rise to a lower number of metastasis when compared to control cells transfected with the vector only. Moreover, mutant RNASET2-expressing cells also displayed a similar or even more increased inhibition of tumorigenicity when compared to wild-type RNASET2, suggesting that catalytic activity is not involved in control of tumor suppression and metastasis.

With the purpose of further defining the biological role of RNASET2, we have undertaken a functional characterization of this gene, by comparing RNASET2-overespressing cells behavior both *in vitro* and *in vivo.* In sharp contrast with previous *in vivo* observations, several *in vitro* tests such as proliferation, clonogenicity, growth in soft agar and apoptosis assays failed to reveal any change in cancer-related phenotypes in the same RNASET2-overexpressing cell line, thus suggesting a non-cell autonomous activity for RNASET2 as a tumor suppressor.
This "asymmetric" *in vivo*/*in vitro* property has been recently ascribed to a novel class of tumor suppressor genes, called tumor antagonizing genes (TAGs), whose oncosuppressive activity is carried out only *in vivo* by induction of microenvironmental remodeling.
To confirm this hypothesis we turned to a xenograft assay and, as expected, Hey3Met2 cells expressing wild-type or mutant RNASET2 were not able to support tumor growth when compared to control mice.
Strikingly, a detailed histological analysis of tumor sections revealed a different architectural pattern between control mice and RNASET2-expressing tumors. The former showed a solid and diffuse growth with strong component of human tumor cells, whereas in the latter a more organized structure and a

massive infiltration of host stromal cells mainly derived from monocyte/macrophage lineage has been found.

In order to establish whether these cells could be functionally responsible for RNASET2-mediated tumor suppression, a further *in vivo* xenograft assay with Rag-2$^{-/-}$ $\gamma_c^{-/-}$ mice was performed, since these mice lack both lymphocytes and NK cells, thus retaining innate immunological response only through macrophages. As previously observed in nude mice, RNASET2-expressing cells were again clearly suppressed in tumorigenicity, further suggesting a functional role for macrophages recruitment in tumor suppression mediated by RNASET2.

To definitively confirm the involvement of this cell lineage, in an additional *in vivo* experiment Rag-2$^{-/-}$ $\gamma_c^{-/-}$ mice were pretreated with the macrophages-depleting agent clodronate before inoculation of Hey3Met2 cells. Untreated mice showed once again a clear effect of tumor suppression exerted by RNASET2 whereas in clodronate-treated mice a very similar tumor development was noticed in both control and RNASET2-expressing cells. Finally, immunohistochemical analysis showed that recruited immune cells mainly belong to M1 subtype of anti-tumorigenic macrophages, suggesting a possible mechanism of tumor suppression exerted by this secreted ribonuclease.

In order to extend RNASET2 functional characterization, beside the experimental model described above a complementary research approach based on gene silencing was carried out, aimed at studying how the lack of RNASET2 could affect tumor development and providing a powerful tool for further investigations.

Our working hypothesis considers RNASET2 inactivation as a critical step in ovarian cancer progression, therefore cancer cell lines endowed with a low *in vivo* tumorigenic potential and expressing high endogenous RNASET2 levels might represent an ideal model system to challenge this hypothesis. In such a context, RNAi-mediated gene knockdown could provide additional information on this topic.

RNAi-mediated silencing of the RNASET2 gene has therefore been attempted in the human ovarian carcinoma cell line OVCAR3, which displays the above mentioned features.

Complete knockdown of RNASET2 in OVCAR3 cell line was successfully achieved and preliminary *in vitro* tests are in keeping with our previous data, showing no significant differences in proliferation and clonogenic potential *in vitro* in RNASET2-silenced when compared to control clones, and further supporting a “non-cell autonomous” behavior of RNASET2.

Gene silencing of RNASET2 also allowed us to studying both the intracellular routing and likely the mechanism(s) by which extracellular RNASET2 affects *in vivo* cell behavior, demonstrating that providing an external source of RNASET2 to silenced OVCAR3 cells resulted in the binding of the ribonuclease to the cell surface and its subsequently internalization.

2. Introduction

2.1 Overview on molecular basis of cancer

A major feature of all higher eukaryotes is the defined life span of the organism, a property that extends to the individual somatic cells, whose growth and division are highly regulated. An exception is provided by cancer cells, which arise as variants that have lost their usual growths control. Their ability to grow in inappropriate locations or to propagate indefinitely may be lethal for the individual organism in which they occur.

The basic model for the occurrence of cancer postulates a multistage process, in which initiation of tumor requires several steps which may then be followed by further changes to strengthen the tumorigenic state. Tumor progression is then driven by selection among the tumor cells for those that can grow more aggressively. Many different types of events are known to contribute to this process at the molecular level. The two major types of changes in the genome of cancer cells are the accumulation of somatic mutations and the development of genetic instability that overall is reflected at the cellular level by an uncontrolled proliferation together with a suppression of apoptosis.

The two classes of genes in which mutations have been linked to cell transformation are oncogenes and tumor suppressor genes.
Oncogenes were initially identified as genes carried by viruses that causes transformation of their target cells. It was found later that a major class of the viral oncogenes have cellular counterparts that are involved in normal cell functions. The cellular genes were called proto-oncogenes, and in certain cases their mutation or aberrant activation in the cell to form an oncogene was associated with tumor formation. The oncogenes fall into several groups, representing different types of activities ranging from transmembrane proteins to transcription factors, growth factors and growth factor receptors, signal transduction proteins, cell cycle regulators and regulators of apoptosis.

The generation of an oncogene represents a gain-of-function event in which a cellular proto-oncogene is inappropriately activated. This can involve a mutational change in a protein's coding region, or a constitutive activation, overexpression, or failure to turn off the oncogene expression at the appropriate time.

Tumor suppressor genes (TSGs) encode proteins whose deletion, repression, expression inactivation, or mutation promotes oncogenesis. In some instances, reactivation of the function of a TSG suppresses the malignant phenotype. This type of TSG usually is referred to as a gatekeeper gene.
Like oncogenes, tumor suppressor genes encode molecules involved in the regulation of cell proliferation. They affect cell cycle regulation, signal transduction, transcription and cell adhesion, and the products of

proto-oncogenes but, unlike oncogenes, tumor suppressor genes act in a recessive manner, requiring in the majority of cases that both copies of alleles are mutated before an effect is manifested.
Inactivation of the other TSGs, namely caretaker genes, leads instead to genomic instability and therefore to an increase in the mutation of other genes that may be gatekeeper genes or influence tumor development. Caretaker genes include those involved in DNA repair or genes that maintain the integrity of chromosomes and their numbers. Unlike gate keeper genes, reconstitution of caretaker genes fails to override these secondary effects and does not suppress malignancy.
Tumor suppressor genes are altered via different mechanism, including deletions and point mutations, which may also result in an inactive or dominant negative product. Regions of chromosomes frequently deleted in tumor cells are thought to harbor TSGs. Often such deletions are easily detectable and provide a means to map the underlying mutant gene. Alternatively, methylation of the promoter of a TSG can down-regulate its expression. Dysregulation of genes encoding proteins that modulate tumor suppressor may also lead to a defect in a given tumor suppressive function. In other examples, chimeric proteins formed by chromosomal translocations can produce dominant negative factors that can decrease expression, stability or function of TSGs.

In a broad sense, any gene that can protect cells from progressing toward neoplastic growth can be considered a TSG, but in recent years several studies suggested that the suppression of cellular growth and the suppression of tumor-forming ability are controlled by different classes of genes (1).
Thus, the canonical definition of TSG could encompass both genes that control cell cycle and proliferation (like p53, RB or that regulate apoptosis) and genes that antagonize with malignancy onset and development, a feature that has a clear meaning *in vivo* but is difficult to translate into *in vitro* contexts (1, 2).
Tumor antagonizing genes (TAGs) have been historically identified from hybrids generated by cell fusion of normal with tumor cells and selected *in vitro* for positive growth and suppression of apoptosis, but *in vivo* they did not produce tumors (3). Moreover, later studies showed that somatic hybrids obtained by single chromosomes transfer from non-cancer cells could suppress tumorigenicity by themselves only *in vivo*, and the reappearance of tumorigenic phenotype was associated in a loss of chromosomal regions that did not harbor the "classical" aforementioned p53 and RB (4, 5).
The most salient feature of TSGs is therefore their ability to suppress tumor growth *in vivo* but not *in vitro*, and as such "asymmetric" behavior could be explained by virtue of complex interactions network that *in vivo* constitute the microenvironmental milieu (cellular and humoral) of the tumor.
A deeper investigation of biology of tumors has indeed clarified that stromal cells that constitute the tumor microenvironmental (fibroblasts, myofibroblasts, endothelial cells, macrophages, lymphocytes) are essential collaborators of the neoplastic process, which can be recruited and exploited by the cancer cell itself (6, 7). Cancer cells generate a supportive microenvironment by producing stromal-modulating growth factors. These include basic fibroblast growth factor (bFGF), members of the vascular endothelial growth factor (VEGF) family, platelet-derived growth factor (PDGF), epidermal growth factor receptor

(EGFR) ligands, interleukins, colony-stimulating factors, transforming growth factor-β (TGFβ) and others. These factors disrupt normal tissue homeostasis, similar to the processes of wound healing, and act in a paracrine manner to induce stromal reactions such as angiogenesis and the inflammatory response. The factors also activate surrounding stromal cell types, such as fibroblasts, smooth-muscle cells, and macrophages, leading to the secretion of additional growth factors and proteases (8, 9, 10).

This general framework means that cancer development is not simply a cell-autonomous process, but represents instead a complex event based on continuous communication between cancer cells and the surrounding non-neoplastic tissue, suggesting that carcinogenesis should be regarded as a tissue disease rather than an individual cell disease (8).

In this context TAGs could take part by interacting with tumor environment (stromal cells, extracellular matrix, soluble signals) and inhibit tumor growth by at least three general processes such as response to differentiation-inducing signals, inflammation signals (eliciting immune response) and angiogenesis inhibition (5).

Among the TAGs recently discovered are HYAL1 and HYAL2, encoding for hyaluronidases (11), and the WWOX gene, which modulates the interaction between tumor cells and the extracellular matrix (12).

2.2 Ribonucleases and cancer

Ribonucleases (RNases) represent an heterogeneous class of evolutionarily conserved enzymes, whose main biological role is involved in RNA metabolism. From a biochemical perspective, RNases degrade RNA through hydrolysis of single-stranded and double-stranded RNAs or RNA-DNA hybrids, but their biological roles include a variety of cellular processes ranging from cytoplasmic or nuclear RNA degradation, RNA processing and editing, gene expression, antiviral defense, angiogenic, neurotoxic and immunosuppressive functions (13).

Furthermore, the most interesting properties include cytotoxic and anticancer activities owned by some classes of ribonucleases, thus placing them as promising alternative to conventional chemotherapy (14); these features are described below with a particular emphasis.

A particular group of ribonucleases are transferase-type RNases, which hydrolyze single-stranded RNA *via* a 2',3'-cyclic phosphate intermediate, forming oligo- or mononucleotides with a terminal 3'-phosphate. They can be classified in several ways, according to substrate or base specificity, optimal pH for activity, cellular localization, origin and sensibility against inhibitors; however the main classification distinguishes between alkaline RNases (with an optimal pH activity of 7.0 and 8.0) which include A and T1 families and acid ribonucleases (pH activity 4.0 to 5.0), belonging to T2 family (15).

Alkaline ribonucleases

Alkaline RNases are characterized by a low molecular weight and an optimal pH for catalytic activity around 7.0-8.0, and are classified into two main subfamilies: RNase A and RNase T1.

T1 RNases are widely distributed in fungi and bacteria, have a molecular mass of about 12 kDa and show cutting specificity for guanine.
Although the most known role for these enzymes is digestive, an important T1 RNase member endowed with anticancer activity is Binase, a 12 kDa bacterial protein isolated from *Bacillus intermedius*.
This enzyme displays a wide spectrum of activities against malignant cells, with selective apoptosis-inducing activity on human myelogen erythroleukemia K562 cells, human lung carcinoma A549 cells and human peripheral blood mononuclear cells (16).

Most information about antitumor ribonucleases came from studies on members of the pancreatic-type ribonuclease superfamily (RNase A family). Enzymes belonging to this family of ribonucleases (which owes its name to the most well-known member, bovine RNase A) are found largely in vertebrate, where

they have mainly a digestive function, a molecular mass ranging between 13 and 14 kDa and cutting preference for pyrimidines (15).

Among these ribonucleases, bovine seminal RNase (BS-RNase), RNase from oocytes of *Rana pipiens* (commercially named Onconase) and two closely related frog RNases from *Rana catesbiana* and *Rana japonica* eggs are of particular interest for their anti-oncogenic activity.

Only in recent years the molecular basis underlying their cytotoxicity is becoming clear. Based on the result obtained so far, a multi-step model has been generally accepted which predicts that cytotoxicity requires these RNases to interact with the cell membrane and to be internalized by endocytosis.

Then cytotoxic RNases are translocated to the cytosol where they cleave cellular RNAs, inducing apoptosis.

The cytotoxic effects and anticancer properties of BS-RNase are well documented (17-20). This RNase shows selective anticancer activity against several tumor cells including thyroid carcinoma cells, 3T3 fibroblast cells (both *in vitro* and *in vivo*), ML-2 myeloid cells and NB-1 and NB-2 neuroblastoma cells. Its selectivity for malignant cells has not been explained yet. Since BS-RNase is endocytosed in malignant and non-malignant cells to the same extent, a different internalization pathway between cancer and normal cells has been proposed (21). To date, no specific receptors have been found for this RNase on the cell surface and it has been suggested that BS-RNase is able to enter cells by adsorption, although involvement of extracellular matrix has been clearly demonstrated (22). Once BS-RNase is delivered in the cytoplasm, its dimeric nature (due to both intermolecular disulfide bonds and non-covalent interaction) prevents its binding to cytosolic ribonucleases inhibitors, increasing cytotoxic activity. The latter is exerted by blocking protein synthesis *via* rRNA cleavage followed by caspases 8/9 mediated apoptosis (17).

Another notable representative member of cytotoxic ribonucleases is Onconase, the smallest member RNase A superfamily, known to be highly cytotoxic to cancer cells (23, 24), and to possess *in vivo* anticancer activity (18). Currently it is under phase III clinical trials for unresectable malignant mesothelioma (14). Onconase works in a similar way to others cytotoxic RNases, acting inside of the cells where it cleaves RNA and trigger apoptosis. Its binding to cell surface in non-saturable way is consistent with the absence of specific receptors, and it was therefore suggested that interaction with plasma membrane occurs electrostatically between negative charges of outer leaflet of cell and positive charges on Onconase surface. Within this frame, it is worth mentioning that cytotoxic RNase obtained by conjugation or fusion of non-cytotoxic RNases to cell membrane ligands, such as transferrin, growth factors or antibodies, are more efficiently taken up by the target cells and, consequently acquired cytotoxic properties (25). Moreover, since the surface of most cancer cells is more electronegative compared to normal cells (26) electrostatic interactions between negative charged cell membrane and positive charges on Onconase surface would be at the basis of its selective anticancer properties.

After internalization by endocytosis, the ribonucleolytic activity of Onconase is allowed by means of both resistance to RNases inhibitor and a high conformational stability due to a pyroglutamyl residue at the N-terminus and a disulfide bridge at the C-terminus. However, the fine mechanism by which Onconase triggers apoptosis is not completely understood and is still controversial (27). It was initially postulated that rRNA and then tRNA whose cleavage causes translational block and thus induces apoptosis were the targets of Onconase. Nevertheless further studies showed that these mechanisms were incompatible with the observed Onconase effects. Indeed, treating cells with a translation inhibitor such as cycloheximide, leads to a complete different pattern of phenotypical and molecular changes compared to Onconase treated cells; moreover Onconase initially induces G1 arrest and apoptosis occurs with a 24-48 hours delay, whereas cycloheximide kills cells indiscriminately in the cell cycle. Finally, the proteins coded by several genes (of which some are involved in regulation in cell cycle progression) are up-regulated after treatment with Onconase. Therefore Zhao and colleagues had suggested that one of the targets of Onconase is the non-coding RNA (microRNAs) that is involved in regulation of gene expression through RNA interference (28).

In human, eight genes encoding catalytically active RNases belonging to the A superfamily (numbered 1 to 8) were identified (29). Despite several information about their biochemical properties are available, the physiological roles of many of them still have to be elucidated.

Among them RNase 5, also called angiogenin, is one of the best characterized enzymes. Angiogenin has a wide tissue and organ distribution and its potent blood-vessel inducing activity suggests that in may play a role in embryologic, neoplastic, inflammatory and immunogenic angiogenesis. Its enzymatic activity as a ribonuclease is essential for angiogenesis; most probably such an activity is performed inside the cell and particularly in the nucleolus, where it is involved in ribosomes biogenesis (30).

Worth mentioning are also RNase 2 and 3, previously known as eosinophil-derived neurotoxin (EDN) and eosinophil cationic protein (ECP), the major secreted proteins of eosinophil granules endowed with antimicrobial, antiviral and antiparasitic activities. Unlike RNase 3, which is an eosinophil specific protein, RNase 2 has also been found in other tissues such as spleen, liver, kidney and placenta and interestingly it has been included in the novel class of proteins called alarmins for its ability to promote maturation and chemotaxis of dendritic cells, contributing to the modulation of both innate and adaptive immunity (31).

Acid ribonucleases

The name “acid RNases” is currently used for two types of RNases in literature.
One type includes pyrimidine base-specific RNases, which are distributed in the vertebrate liver, spleen, urine, monocytes, and other tissues. They have a primary structure similar to RNases A and due to optimal pH activity of 6.5 – 7.0 they are referred as “weakly acid” ribonucleases (15).

To the other type of acid RNases belongs the Rh/T2/S family, with an optimal pH of 4.0 – 6.0 (thus are considered “real acid” RNases) and a molecular weight between 20 kDa and 40 kDa.
Rh/T2/S ribonucleases are secreted glycoproteins represented in most organisms across kingdoms, being widely distributed in protozoans, plants, bacteria, animal and viruses. The name of the family (often simply referred as “T2”) derived from the most studied ribonucleases within this family which include RNase Rh of *Rhizopus niveus*, RNase T2 from *Aspergillus oryzae*, and S-glycoproteins isolated in higher plants. Depending on the organism they are found, they are involved in various functions such as role in the pathogenesis, phosphate remobilization, defense against pathogens and self-incompatibility in plants (15). As well as ribonucleases A-type, they catalyze the cleavage of single stranded RNA through a 2’,3’-cyclic phosphate intermediate, producing mono- or oligonucleotides with a terminal 3’ phosphate group.
A shared important feature of all Rh/T2/S glycoproteins is the presence of two highly conserved common motives named CAS I and CAS II (Conserved Active Site segment), harboring the catalytic activity. In CAS I (IHGLWP) and CAS II (KHGTC) amino acid residues critically involved in the catalytic activity (such as His 46, His 104, His 109 and Glu 105 in RNase Rh numbering) are located (32). Moreover, four cysteine residues forming disulfide bonds are common to all RNases of T2 family, conferring to Rh/T2/S RNases a very compact and stable structure.
The majority of the T2 family RNases are glycoproteins, showing a wide range in their carbohydrate content. In general, N-glycosylation occurs at the consensus sequence Asn-X-Thr/Ser (O-glycosylation is rare) and in most cases the glucidic moiety is made up of glucose, mannose and glucosamine (32).
Due to the widespread diffusion in all organism, RNase T2 functions and cellular localization are very different.
In fungi, extracellular T2 RNases are reported to have a role in nutrition by scavenging nucleotides and phosphate for growth and metabolism. In higher plants an analogous activity has been reported, since phosphate starvation causes an increase of S-like RNases localized in vacuole and extracellular environmental. Secreted RNases scavenge extracellular RNA and recycle its components to the cell, whereas vacuolar RNases also function in recycling of cytoplasmic RNAs that are delivered to the vacuole/lysosome during autophagy (33).
Another interesting function is associated to stylar S-RNases, known for their role in gametophytic self-incompatibility (a system through which genetically related-pollen is recognized and rejected prior to fertilization) and isolated from members of Solanaceae, Rosaceae, and Scrophulariaceae. These

extracellular S-RNases are pistil proteins that are secreted into the extracellular matrix and enter in both incompatible and compatible pollen tubes.

The pistil then distinguishes between self and non-self pollen, based on whether or not the S-allele of the haploid pollen matches either of the two S-alleles of the diploid pistil and matching results in rejection. S-RNases are secreted by ovary cells and act as cytotoxins: they enter the pollen tube cytoplasm and interact with SLF, an F-box domain that contains proteins able to mediate polyubiquitination. In a compatible pollination, non-self interaction leads to S-RNase degradation by the 26S proteasome; otherwise, in an incompatible pollination S-RNases evade SLF control and degrade rRNA, inhibiting the growth of self-pollen tubes (34).

Another example of T2 RNases with cytotoxic activity comes from classical swine fever virus (CSFV) (33). In this virus, one of the envelope glycoproteins, termed E^{rns}, has an RNase T2 domain and ribonuclease activity, and is secreted by infected cells. *In vitro*, this enzyme produces a selective cytotoxic effects against lymphocytes, suggesting that virally infected cells secrete E^{rns} to reduce the host immune response.

Interestingly, some T2 RNases seem to play a biological role in a catalytic-independent manner.

In yeast (35), during oxidative stress Rny1p (homologous to the human RNASET2 gene) is released from the vacuole and cleaves cytoplasmic tRNAs and rRNAs, by means of its catalytic activity. Nevertheless, Rny1p also modulates yeast cell survival during oxidative stress, resulting in reduced cell viability and apoptosis, and this role is apparently carried out irrespective of the ribonucleolytic activity of the protein. Therefore the authors suggested that cellular response to stress involves two parallel pathways, in which release the vacuolar Rny1p functionally mimics cytochrome c release from mitochondria in higher eukaryotes.

Another T2 ribonuclease that exhibits a catalytic-independent function is ACTIBIND, the extracellular RNase purified from *Aspergillus niger*. Unrelated to its RNase activity, ACTIBIND binds *in vitro* actin filaments, resulting in altered actin organization and cell morphology that in turn is reflected in reduced colony formation and motility of several tumor cell lines. *In vivo* it inhibits growth and metastasis in colon cancer and melanoma mouse model (36, 37) and shows angiogenesis inhibition both *in vitro* and *in vivo*, by competing with angiogenin.

2.3 The human ribonuclease RNASET2

The peritelomeric region of the long arm of human chromosome 6 has been intensely investigated in recent years in order to find putative tumor suppressor genes. Indeed, a wide range of solid and hematological neoplasia, ranging from carcinomas of the ovary, breast, uterus, melanoma, non-Hodgkin B-cell lymphoma and acute lymphoblastic leukemia have been associated to rearrangements and deletions in this region (38-43). Among the solid tumors, ovarian cancer has been deeply studied, because of mortality rate, mostly due to late diagnosis; moreover, little is known about the genetic pathways underlying its development. By employing LOH analysis with markers located on the long arm of chromosome 6, three consensus regions of loss of genetic material have been identified, namely 6q21-23.3, 6q25.1-25.2 and 6q26-27 (44-46). In the latter region, later studies revealed the minimal chromosome region found deleted in ovarian tumors, flanked by markers D6S193 and D6S297 (47-49). Between these two markers, in a region that spans about 27 Kb maps the RNASET2 gene, coding for the only known human Rh/T2/S ribonuclease (50).
RNASET2 is present in the human genome as a single copy gene, organized into nine exons and eight introns, and is expressed in almost all normal tissues, such as liver, ovary, lung brain, heart, placenta, kidney and skeletal muscle (50).

The first indications for RNASET2 involvement in ovarian cancer came from gene expressions studies performed on many primary ovarian tumors, already known to contain 6q26-qter deletions in at least one of the chromosome 6 homologues. Decreased RNASET2 transcript levels where found in 30% of them, but neither inactivating mutations in the coding sequence, intron-exon boundaries, 5' and 3' flanking regions nor abnormally methylated CpG in the promoter region were detected, thus indicating a class II tumor suppressor behavior for this gene (50).
A more direct evidence for RNASET2 control of tumor growth was subsequently obtained by transfecting RNASET2 cDNA in the ovarian cancer cell line Hey4 and testing for its ability for tumor formation in nude mice, showing a strong tumor growth inhibition (50).
Remarkably, further *in vivo* characterization revealed that catalytic activity was dispensable for tumor and metastasis suppressions. In this study, athymic mice were injected with a highly metastatic ovarian Hey3Met2 cell line stably transfected with RNASAET2 wild-type or catalytically inactive mutant, obtained by means of substitution of amino acids critically involved in catalysis. Wild-type RNASET2-expressing cells formed smaller tumors in mice and gave rise to a lower number of metastasis with respect to control cells transfected with the vector only. Moreover, mutant RNASET2 also displayed a similar or even more increased inhibition of tumorigenicity when compared to wild-type RNASET2, suggesting that ribonuclease activity is not involved in control of tumor suppression and metastasis (51).

The RNASET2 gene encodes for an extracellular glycoprotein of 256 amino acids with a predicted molecular weight of 30 kDa. The protein contains a signal peptide for secretion at the N-terminal and three N-glycosylation sites are predicted to occur at positions 76, 106 and 212, increasing the molecular weight of about 6 kDa. Like other Rh/T2/S glycoproteins, two highly conserved CAS segments are found in RNASET2, ranging from position 65 to 69 and from position 117 to 121 (figure 1).

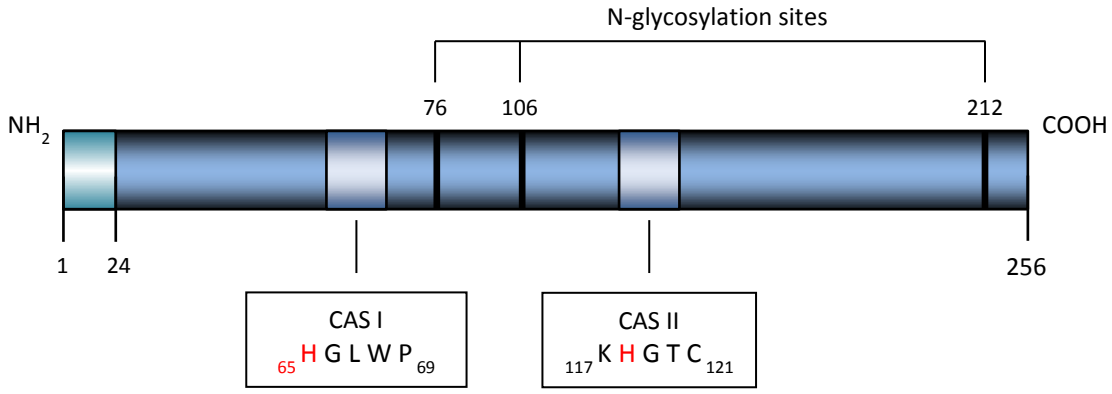

Figure 1. RNASET2 protein structure

Full length RNASET2 is characterized by a signal peptide located at N-terminal position, (ranging from amino acid 1 to 24), two active site segments (CAS I and CAS II) highly conserved among T2 family ribonucleases and three N-glycosylation sites bioinformatically predicted at positions 76, 106 and 212. In the RNASET2 H65/118F mutant, two essentials histidines (red letters) for catalysis are substituted with two phenylalanines, leading to a catalytically inactive form.

In cell lysates RNASET2 is present in three forms of different sizes, namely 36, 31 and 27 kDa. The 36 kDa isoform represents the full-length and secreted form, whereas the other two isoforms likely originate from proteolytic cleavage occurring at C-terminal. All three forms are glycosylated, since treatment of intracellular lysates with PNGase F resulted in a proportional shift toward a lower molecular weight (36, 31, and 27 kDa forms shifted to 31, 23 and 19 kDa respectively) (52).

Subcellular fractionation followed by immunoblot revealed that the RNASET2 full-length form is enclosed in the endoplasmic reticulum, while the two proteolytic forms were detected in the lysosomal fraction, indicating that RNASET2 is targeted as a full-length form to the secretory pathway but undergoes proteolytic cleavage during transport or delivery to the lysosome. The catalytic activity has also been investigated, showing that RNSET2 cleaves with an optimal pH at 5 either total RNA or tRNA and glycosylation is not required for catalysis. In contrast with most members of Rh/T2/S family, some base specificity has been reported since poly-U and poly-A oligonucleotides were preferentially cleaved compared to poly-G and poly-C (52).

3. Results

3.1 *In vitro* cell based assays

In a previous work, RNASET2 has been defined as a candidate oncosuppressor gene by means of its ability to suppress tumor growth *in vivo* once overexpressed in the highly oncogenic and metastatic Hey3Met2 ovarian cancer cell line (51). Such tight control of *in vivo* tumorigenesis raised the question whether RNASET2 could exert its antitumorigenic role in a cell-autonomous manner, as already described for other tumor suppressor genes.

For this purpose, several in *vitro* test were performed, by comparing a wide range of cancer-related phenotypes in RNASET2-overexpressing cells compared to Hey3Met2 control clones.

Four stable transfected control clones carrying the pcDNA3 empty vector and eight RNASET2-expressing stable transfected clones with the same level of expression of RNASET2 wild type or H65/118F mutant (four per group, figure 2) were analyzed in triplicate for each *in vitro* assay.

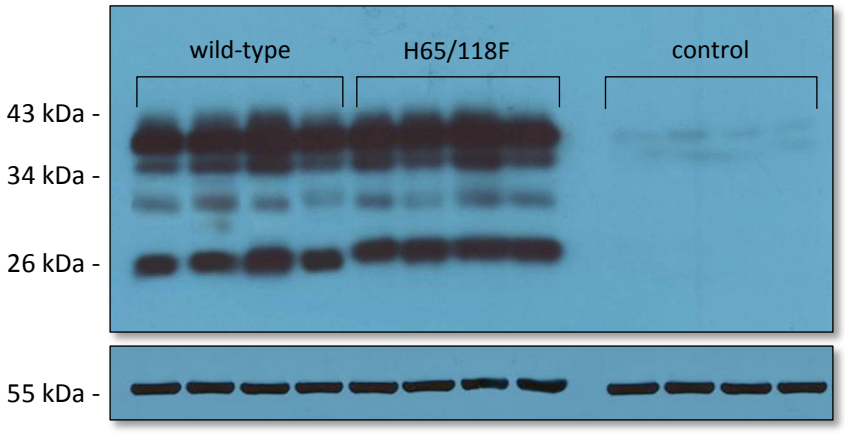

Figure 2. Immunoblot probed with polyclonal antibody anti-RNASET2

Upper panel: intracellular lysates of Hey3Met2 are checked for RNASET2 expression. Control clones show a very low level of endogenous expression.

Lower panel: the same blot was probed with anti-α-tubulin monoclonal antibody for normalization.

The first parameter analyzed was the cell growth kinetic, in order to assess if the strong RNASET2-mediated tumor suppression observed *in vivo* could depend on reduced proliferation rate.

Four Hey3Met2 clones were plated in triplicate in a 24 well culture plate for each construct (namely pcDNA3 empty vector, pcDNA3-RNASET2 wild type or pcDNA3-RNASET2 H65/118F mutant) and growth was followed for 8 days.

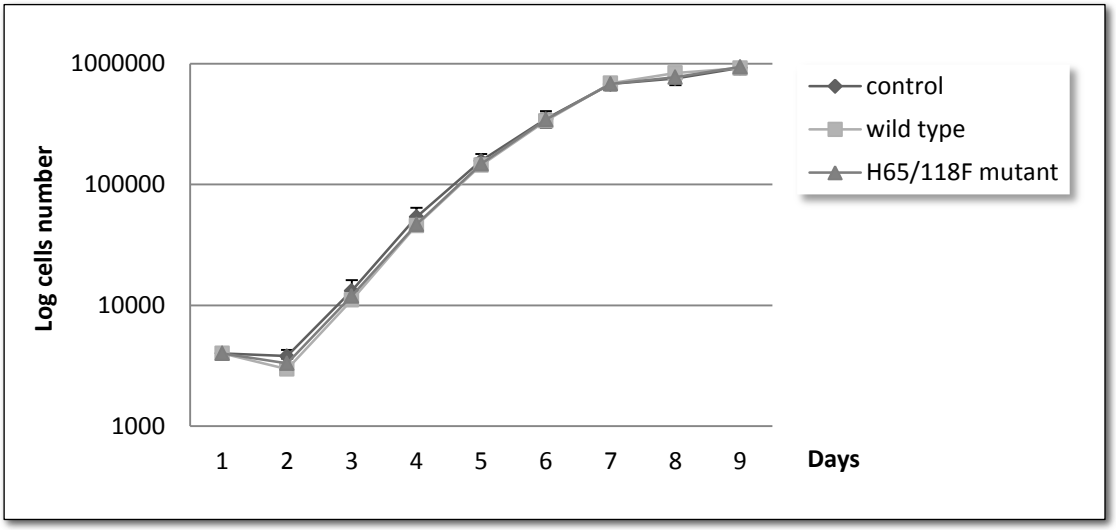

Figure 3. Growth curve

The graph represents the mean of values of each group of clones. Rumble: pcDNA3 vector; squares: pcDNA3-RNASET2 wild type; triangles: pcDNA3-RNASET2 H65/118F mutant. Bars indicate the standard error.

As shown in figure 3, we could not detect any statistically significant difference in the proliferation kinetic among the analyzed clones.

From these raw data, the population doubling time was also calculated, resulting in almost identical values for all experimental conditions (figure 4).

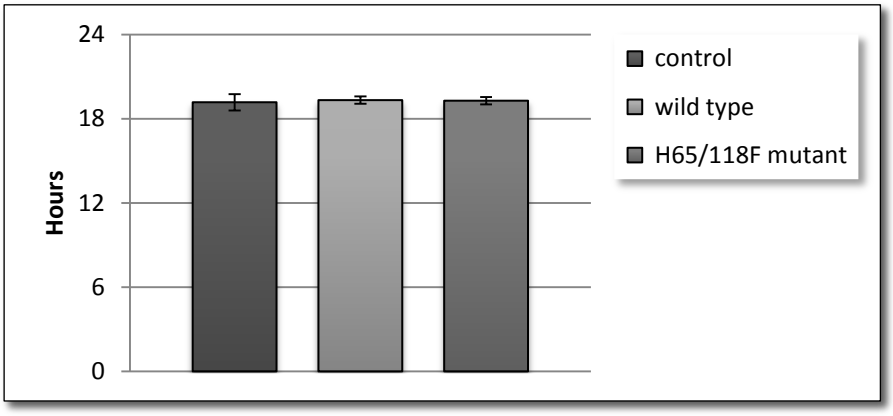

Figure 4. Doubling time

The mean of doubling time for each group of clones is 19 hours, with only few tens of minutes of difference between them. Bars indicate the standard error.

Although the analysis of growth curve kinetics ruled out any difference between RNASET2-expressing and control clones, this kind of test simply describes a steady state of total cells number in culture, and is therefore not informative about dynamic events affecting cell behavior *in vivo* or *in vitro*.

Such processes, like proliferation and apoptosis, could balance their opposite effects so that cells in culture apparently grow to the same extent but have very different behaviors in relation to these two parameters. To examine this possibility, bromodeoxyuridine (BrdU) incorporation and TUNEL apoptosis assays were carried out on the same cell clones previously investigated (figure 5 and 6).

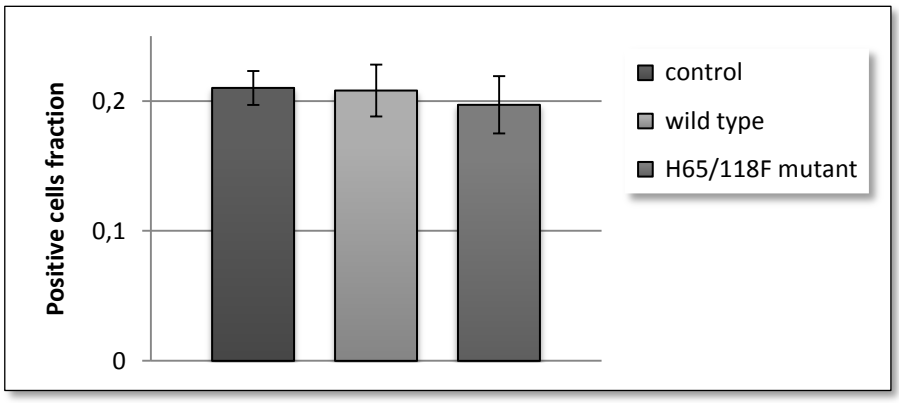

Figure 5. BrdU incorporation

Actively proliferating cells incorporate BrdU as thymine analog during DNA synthesis and then are labeled with specific antibody. Positive cells are then manually counted by microscope. Bars indicate the standard deviation.

The bromodeoxyuridine incorporation assay revealed that all clones were proliferating to the same extent, with a fraction of proliferating cells of about 20%. The same result was obtained when apoptosis rates were investigated, with only minimal differences between RNASET2-expressing and control clones.

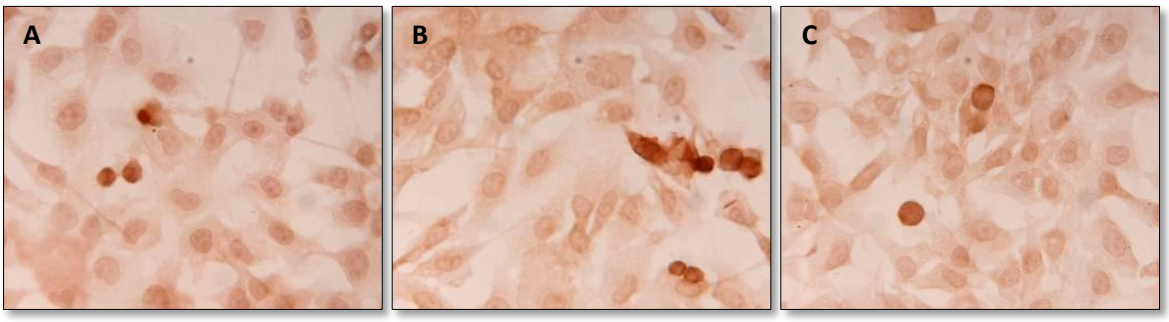

Figure 6. TUNEL apoptosis assay

Cells are seeded on coverslips and the day after are fixed in paraformaldehyde. After permeabilization TdT reaction is detected by streptavidin-HRP conjugated, by using DAB as chromogenic substrate.

In the reported images dark brown cells are apoptotic ones. The percentage of apoptosis is around 3% for each clone.

A – pcDNA3 vector; B – pcDNA3-RNASET2 wild type; C – pcDNA3-RNASET2 H65/118F mutant.

The results from both proliferation rate and apoptosis assays showed no statistically significant differences among the different experimental groups, indicating that RNASET2 actually does not affect the rate of cell growth *in vitro.*

Within solid tumors, very often only a small fraction of the cells are actively proliferating (hence giving rise to colonies), and so are directly responsible of the tumor growth (53). To investigate the effect of RNASET2 on the colony-forming ability of Hey3Met2 cells, an *in vitro* clonogenic assay was performed, but differences in neither colony number nor size were detected in Hey3Met2 RNASET2-expressing and control clones (figure 7).

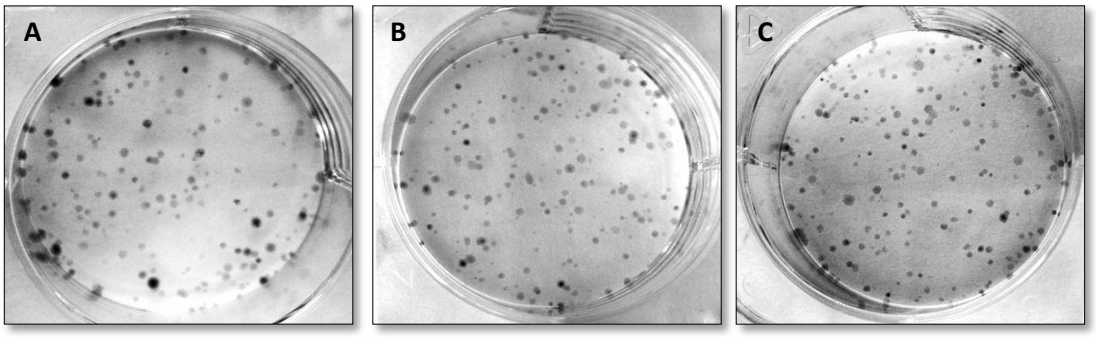

Figure 7. Clonogenic assay

Cells were plated in 6-well culture plates (2 x 10^2 cells per well) and following 14 days incubation, clones were stained with a methylene blue solution (1% methylene blue, 50% ethanol) and visible colonies were manually counted.

A – pcDNA3 vector; B – pcDNA3-RNASET2 wild type; C – pcDNA3-RNASET2 H65/118F mutant.

As an independent parameter to evaluate the transformed phenotype of RNASET2-expressing cells, anchorage-independent growth was also investigated. A typical feature of malignant cancer cells involve their ability to growth *in vitro* without adhering to a solid substrate. Indeed, transformed cells not only lose contact inhibition with neighboring cells to form foci, but also gain the ability to growth in anchorage-independent manner. This parameter can be easily tested by measuring the growth of isolated cancer cell colonies in soft agar, a semi-solid medium that usually does not support the growth non-cancer cells. When this assay was carried out with the Hey3Met2 clones, even though a slight variability among different clones transfected with the same construct was observed, no significant differences were once again found among Hey3Met2 control and RNASET2-overexpressing clones (figure 8).

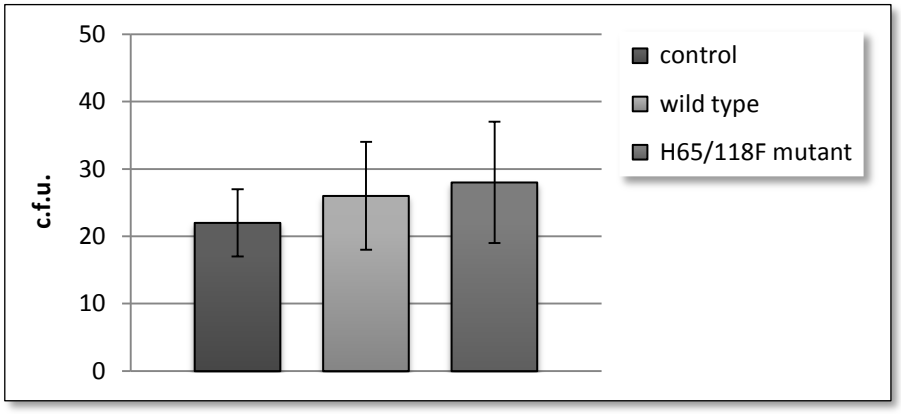

Figure 8. Soft agar growth

To evaluate anchorage-independent growth, a two-layers soft agar test was performed. For each clone 100 cells were resuspended in 0.3% Bacto-Agar in DMEM F12 supplemented with 20% FBS and then plated over a layer of 0.6% Bacto-Agar in DMEM F12 supplemented with 20% fetal bovine serum in 12 well culture plates. Colonies were counted after 14 days. Bars indicate the standard deviation.

Finally, RNASET2 was tested for its ability to mediate cell adhesion to an artificial membrane preparation (Matrigel), since a clear connection between tumor cells adhesion to the extracellular matrix and invasive and metastatic behavior has long been established (54). As shown in figure 9, the effects of RNASET2 were unremarkable for this parameter as well.

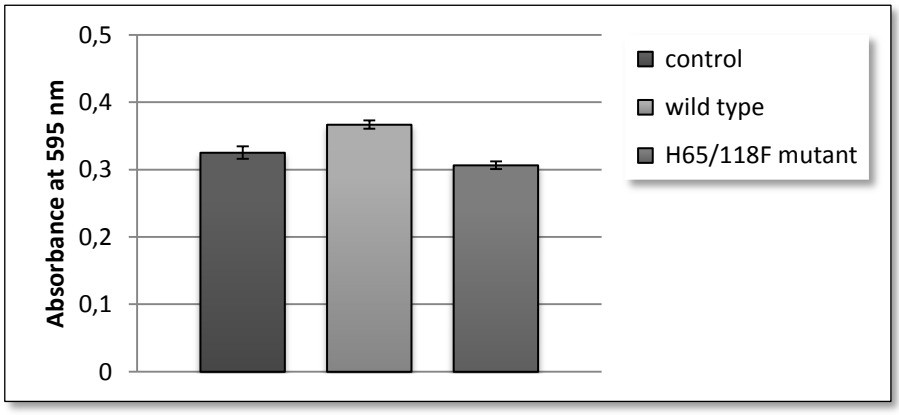

Figure 9. Adhesion test

Cells were plated on non-tissue culture plate previously coated with matrigel ($5x10^3$ cells/clone, 10 wells/clone). After 4 hours of incubation the adhering cells were stained with crystal violet and absorbance value measured. Bars indicate the standard error.

Collectively, the results from this wide range of *in vitro* assays convincingly showed that RNASET2 does not influence any cancer-related parameter *in vitro*, thus suggesting a non-cell autonomous role for this gene.

In this view, apparently RNASET2 is not able by itself to control the tumorigenic phenotype in the cellular context in which it is expressed, but would instead require a broader context of interactions, such as those that can be established *in vivo* between cancer cells and the tumor microenvironment.

Subsequent investigations were therefore focused to this topic, with the aim to characterize the antitumorigenic role of RNASET2 in *in vivo* experimental system.

3.2 Analysis of tumors from *in vivo* experiments on athymic mice

With the aim to better define the role of RNASET2 *in vivo*, a xenograft assay was carried out by inoculating in nude mice the same Hey3Met2 clones previously characterized *in vitro*. Thereafter, a detailed histological and immunohistochemical analysis of tumor specimens was performed. In keeping with our previous *in vivo* experiments, large tumors developed in control mice inoculated with Hey3Met2 clones transfected with the empty vector, whereas RNASET2-expressing clones showed a negligible increase in the tumor mass over time (figure 10). Moreover, mutant RNASET2-expressing clones were even more suppressed in tumorigenicity than wild-type expressing clones, thus further confirming our previous observation that the catalytic activity of RNASET2 is not required for tumor suppression.

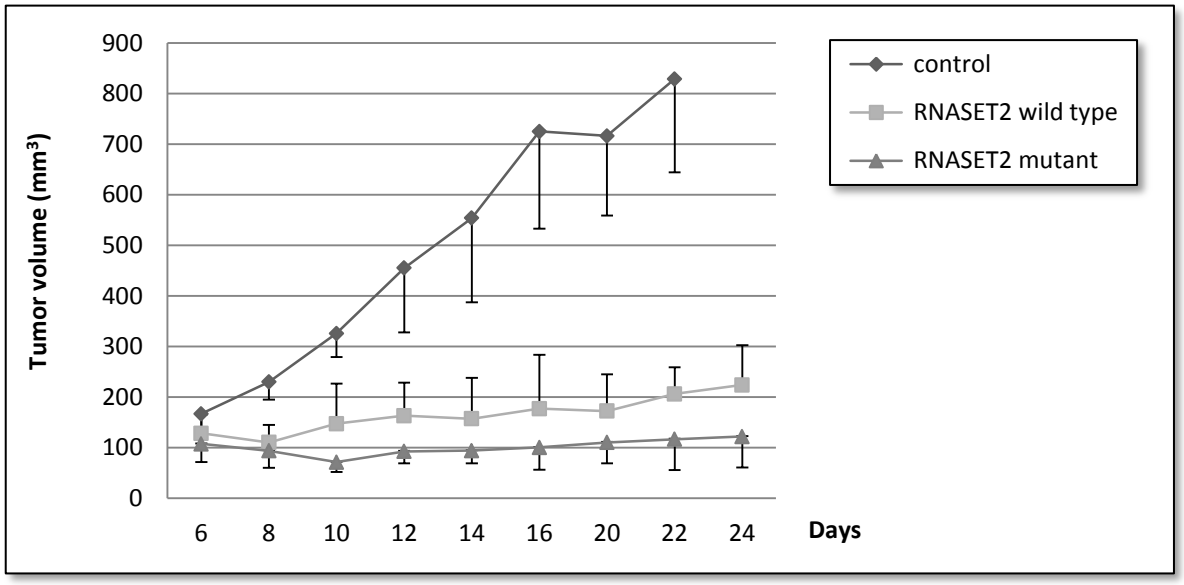

Figure 10. Tumorigenicity test *in vivo* by xenograft in nude mice

Hey3Met2 clones ($5x10^6$ cells/clone) stably transfected with pcDNA3 control plasmid, wild type or mutant RNASET2 were grafted by subcutaneous injection in athymic mice (5 mice/clone) and tumor growth was checked every two days. Bars represent the standard deviation values.

To better investigate the cellular and molecular mediators of RNASET2-dependent tumor suppression, tumour specimens from the xenograft assay were isolated, formalin-fixed and paraffin-embedded for histological and immunohistochemical analysis.

We first verified that RNASET2 expression was maintained *in vivo*. To this end, an immunohistochemical (IHC) assay was carried out by immunostaining tumor sections with an anti-RNASET2 polyclonal antibody (figure below).

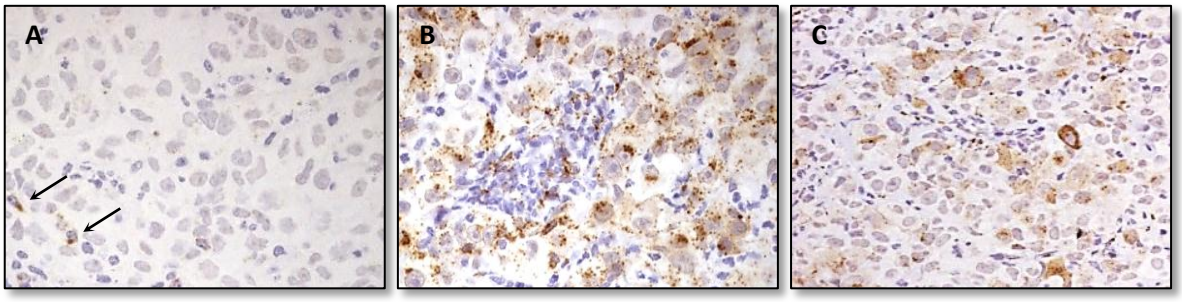

Figure 11. RNASET2 is maintained in tumors sections

Immunohistochemistry with anti-RNASET2 on tumours from athymic mice inoculated with Hey3Met2 transfected with vector only (A) or with constructs expressing wild-type (B) or mutant (C) RNASET2. Original magnification 100X.

As shown in figure 11, control tumors showed an expected weak staining (arrows, image A), in keeping with the very low endogenous RNASET2 expression levels of Hey3Met2 cells. By contrast, the RNASET2 protein was clearly detectable in sections from tumors inoculated with cells transfected with both RNASET2 expression vectors, showing a granular signal in the cytoplasm of tumour cells which likely represents the secretory compartment.

We next investigated the morphological features of RNASET2-expressing and control tumors sections.
Hematoxylin and eosin staining (H&E, figure 12) showed that all tumors were characterized by the presence of two main cell populations with a different nucleus/cytoplasm ratio and basophilic affinity.
Control tumors were characterized by a rather homogenous architecture, being made of a predominant population characterized by big cells with low nucleus/cytoplasm ratio (likely representing cancer cells) with only few cluster of intensely stained small cells of probable murine origin.
By contrast, in RNASET2-expressing tumors a complete different tissue architecture was found, with the tumor mass sepimented by an abundant infiltrate of smaller intensely stained cells arranged in cordon-like structures.
Moreover, in both wild-type and mutant RNASET2-expressing tumors a Masson's trichrome staining showed that neoplastic cells were surrounded by bridges of accumulated connective tissue containing an increased population of smaller cell (figure 13).

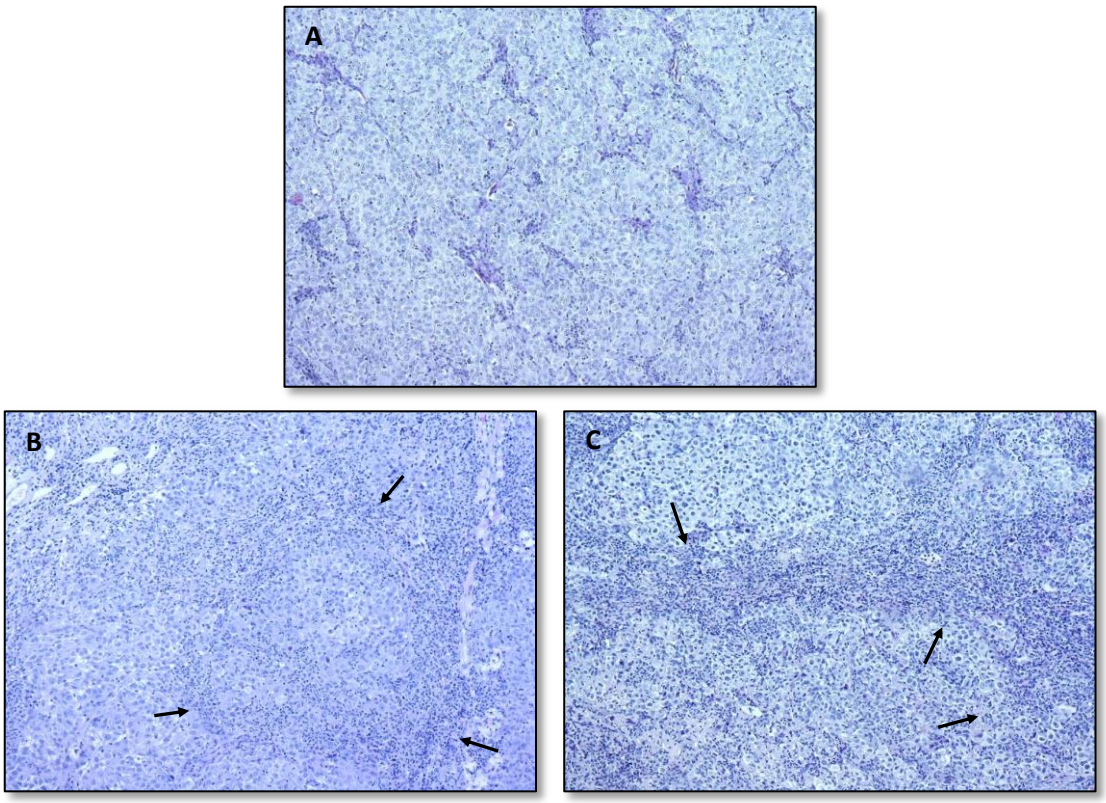

Figure 12. H&E staining reveals different tissue architecture among tumors

Two main cell populations with can be distinguished, according to size and different staining. Furthermore, homogeneous and compact structure can be noticed in control tumors (A) whereas cordon-like structures (arrows) of host cells can be clearly see in RNASET2-overexpressing tumors (wild type, B, and mutant, C). Images are representative of multiple fields analyzed in at least six sections derived from tumors excised in three independent animals for each experimental group. Original magnification 40X.

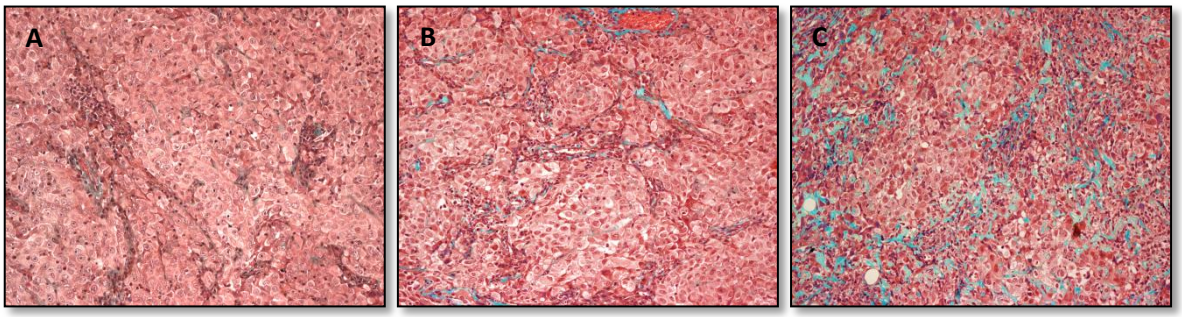

Figure 13. Masson's trichrome staining

In wild type and mutant RNASET2-expressing tumors (B and C respectively) neoplastic cells are surrounded by connective tissue (stained in blue), whereas in control tumors (A) such component is absent. In the former tumors, between collagen fibers, a more intense staining of nuclei and cytoplasm reveals a population of host-derived cell, whose morphological analyses indicated to be mostly granulocytes and mononuclear cells. Original magnification 40X.

Taken together, these data suggested that RNASET2-expressing tumors were associated with a massive cellular infiltrate derived from the host stromal compartment, and prompted us to better investigate this cell population.

In order to verify that the infiltrating cell population observed in tumor sections was of murine origin, a chromogenic in situ hybridization (CISH) assay was performed by using a murine chromosome Y-specific centromeric probe. This probe allowed us to identify only murine cells, since the inoculated human cancer cells were derived from ovarian carcinoma whereas the recipients mice were males.

Strikingly, the CISH assay clearly demonstrated that the cell population infiltrating the tumors was derived from the mouse host stromal compartment (figure 14).

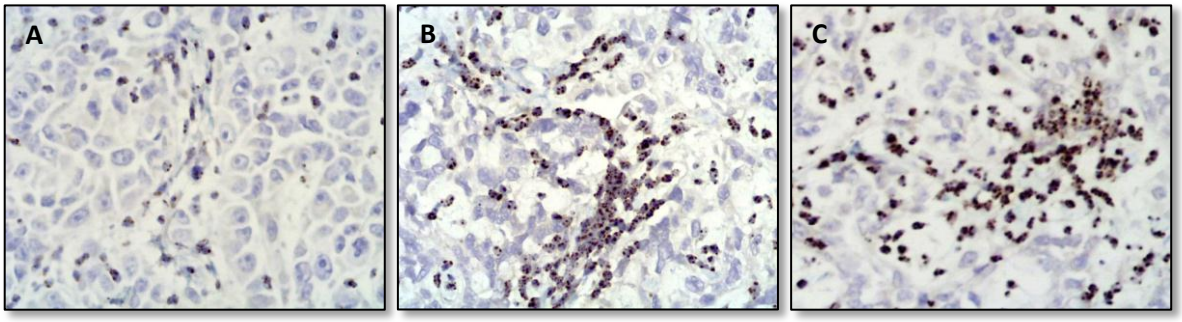

Figure 14. Chromogenic in situ hybridization (CISH) reveals host-derived origin of infiltrating stromal cells

A – control tumor; B – wild type RNASET2-expressing tumor; C – mutant RNASET2-expressing tumor. Original magnification 100X.

Since a preliminary morphological analyses suggested that the host stromal cells segregating in connective strands within the neoplastic mass in RNASET2-expressing tumors might belong to the granulocytes/mononuclear lineage, an immunohistochemical assay was carried out to detect the CD11b antigen, (a component of the CD11b/CD18 integrin heterodimer that is expressed in natural killer cells, monocytes and granulocytes) and the F4/80 antigen (figure 15 A'-C'), a cell surface glycoprotein restricted to mature macrophages and therefore absent in granulocytes and lymphocytes.

For both markers, a few reactive cells were detected in control tumors when compared to RNASET2-expressing tumors, where a massive population of strongly reactive cells infiltrating the tumors (mostly represented by cells from the monocyte/macrophages lineage) was detected, (figure 15, A-C and A'-C').

On the basis of these data, we established a novel working hypothesis by which RNASET2 could carry out its tumor suppressing activity by stimulating a massive recruitment into the tumor mass of cells from the host immune system, which in turn might contribute to tumor growth suppression.

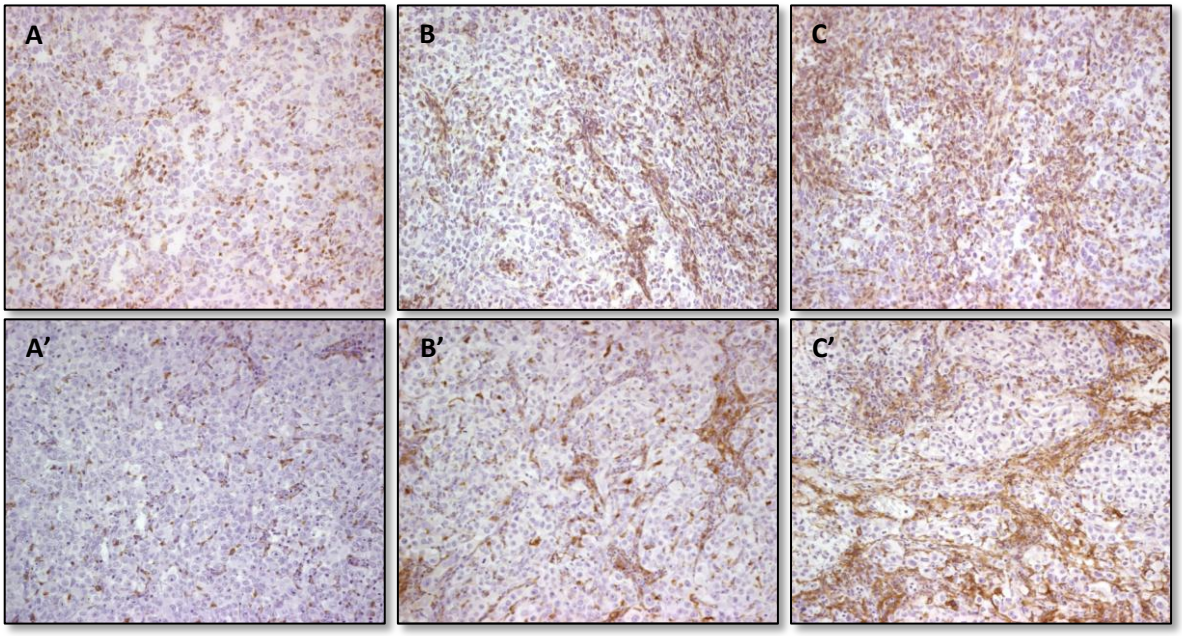

Figure 15. Characterization of host infiltrating cells

Upper panel: immunohistochemistry with anti-CD11b.

Lower panel: immunohistochemistry with anti-F4/80.

A massive infiltration of host immune system cells is detected in RNASET2-expressing tumors (brown spots)

A, A' – control tumor; B, B' – wild type RNASET2-expressing tumor; C,C' – mutant RNASET2-expressing tumor. Original magnification 40X.

Having defined the cell population infiltrating RNASET2-expressing tumors, we then shifted our attention to the putative mechanisms behind RNASET2-mediated tumor suppression. To this aim, three main processes were investigated such as proliferation rate, apoptosis and vascularization.

Tumor specimens were thus analyzed by immunohistochemistry with antibodies raised against activated caspases 3 (cleaved caspases 3, CCL-3), Ki-67 (a nuclear non-histonic protein expressed only by proliferating cells) and CD31, a specific component of endothelial cell junctions.

As shown in figure 16, the majority of cells in control tumours were actively proliferating, whereas in RNASET2-expressing tumours (and particularly in those expressing the mutant form) a decreased proliferation rate was observed.

By contrast, an opposite pattern was observed for CCL-3 staining, with an increased number of positive cells detected in wild-type, and even more in mutant-RNASET2 expressing tumors with respect to control tumors.

Finally, in clear contrast to these observations, no apparent changes in blood vessel density and morphology could be observed between RNASET2-transfected tumors and controls.

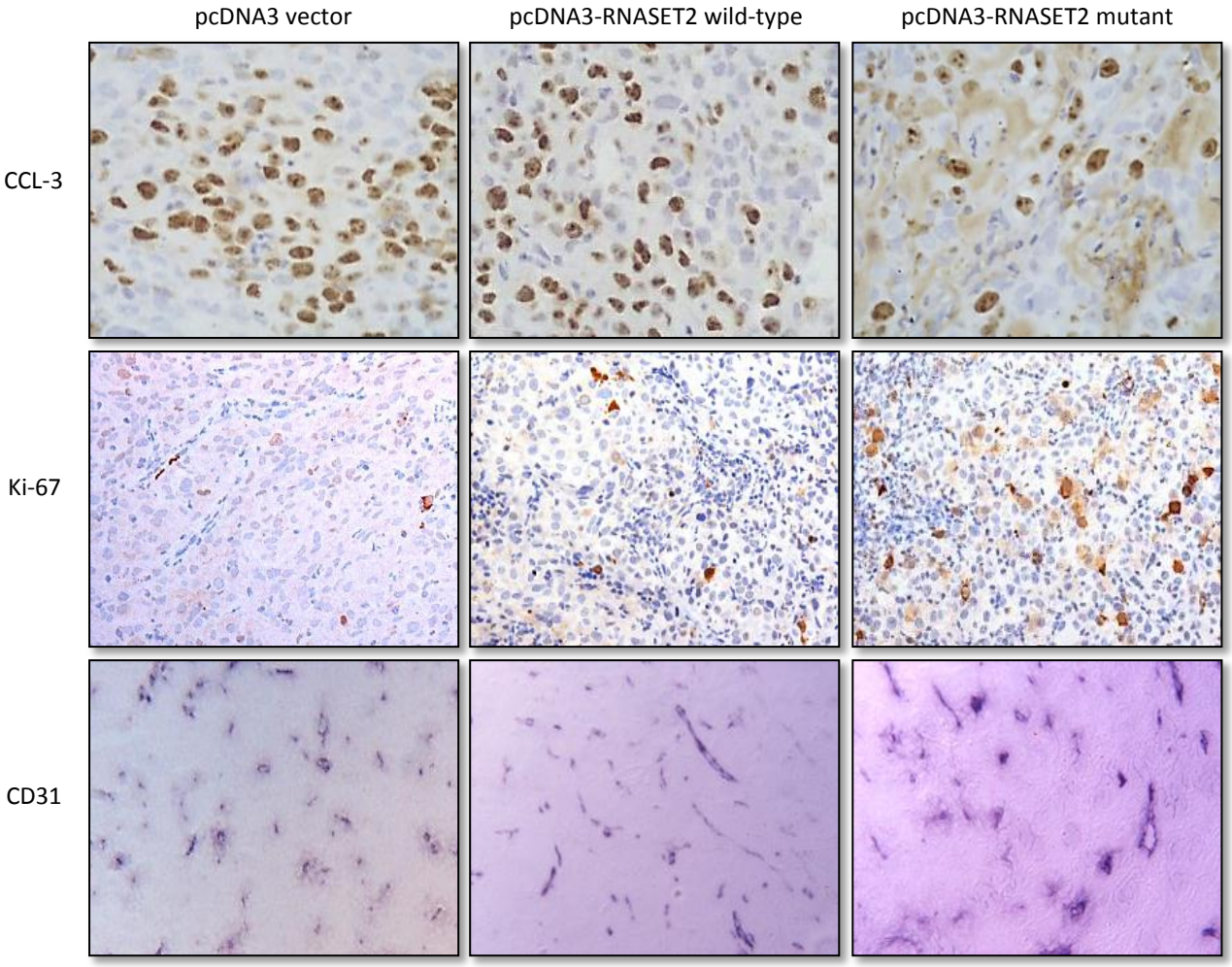

Figure 16. Immunohistochemical detection of apoptotic, proliferating and endothelial cells in tumor samples

Upper panel: immunohistochemistry with anti-active caspases 3 (original magnification 100X).

Middle panel: immunohistochemistry with anti-Ki-67 (original magnification 40X).

Lower panel: immunohistochemistry with anti-CD31 (original magnification 40X).

Photomicrographs shown are representative images of multiple fields examined in at least four sections derived from tumor excised in two to three independent animals for each experimental group.

3.3 Analysis of tumors from *in vivo* experiments on Rag-$2^{-/-}$ $\gamma_c^{-/-}$ mice

The experimental data just described, obtained in an athymic mouse model, strongly suggest that macrophages might play a critical role in control of RNASET2-mediated tumor suppression.
In order to better define the functional role of this cell population, a new experimental model based on Rag-$2^{-/-}$ $\gamma_c^{-/-}$ mice has been carried out.
These mice are devoid of lymphocytes, due to a mutations that inactivates the Rag genes (Recombination-Activating Gene) encoding for key components of the lymphoid-specific recombinase. Moreover, a second mutation has been introduced in the gene coding for the "common γ chain" (γ_c) of many hematopoietin receptors, essential for the maturation and survival of lymphocytes, mast cells and NK-cells. As a result of these mutations, Rag$2^{-/-}$ $\gamma_c^{-/-}$ mice are endowed with a partial innate immune system response, represented by the monocyte-macrophage and granulocyte cell population.
In a trial experiment, Hey3Met2 clones were grafted in Rag-$2^{-/-}$ $\gamma_c^{-/-}$ mice and, as shown in figure 17, tumor development was strongly impaired in mice injected with RNASET2-expressing cells, whereas control tumors reached a tumor mass of 1300 mm^3 in 19 days only. Thus, *in vivo* suppression of tumor growth carried out by RNASET2 irrespective of its catalytic activity was confirmed in a second independent xenograft model.

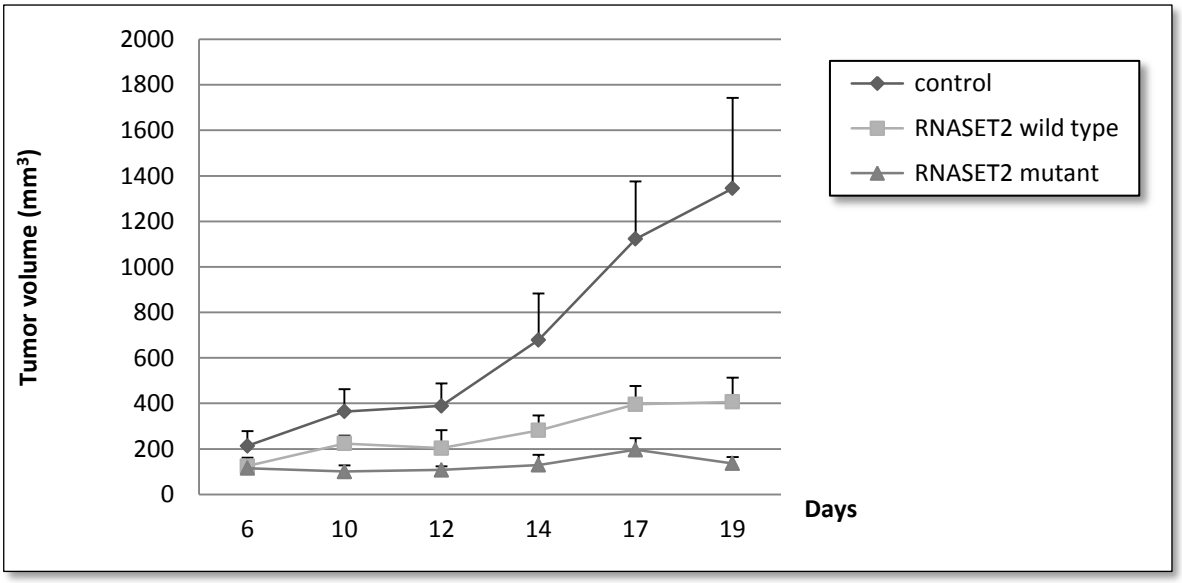

Figure 17. Tumorigenicity test *in vivo* by xenograft in Rag-$2^{-/-}$ $\gamma_c^{-/-}$ mice

Hey3Met2 clones stably transfected with control plasmid or RNASET2-expressing vectors were grafted by subcutaneous injection into Rag-$2^{-/-}$ $\gamma_c^{-/-}$ mice (3 mice per clone) and tumor growth was checked every two day until day 19.
Bars represent the standard deviation values.

To definitively confirm the involvement of macrophages, in a further *in vivo* experiment Rag-$2^{-/-}$ $\gamma_c^{-/-}$ mice were treated with the macrophages-depleting agent clodronate before injection of Hey3Met2 clones.

Clodronate (figure 18) is a non-toxic drug that accumulates intracellularly into phagocytic cells once delivered using liposomes as vehicles.

Lysosomal phospholipases within phagocytic cells hydrolyze the phospholipid bilayers of the liposomes and clodronate is then released into the cell, where it rapidly accumulates until a threshold concentration is reached, after which the cell is irreversibly damaged and dies by apoptosis (55).

By contrast, free clodronate, such as that released from dead macrophages, has an extremely short half-life in the circulation and is quickly removed from the circulation by the renal system.

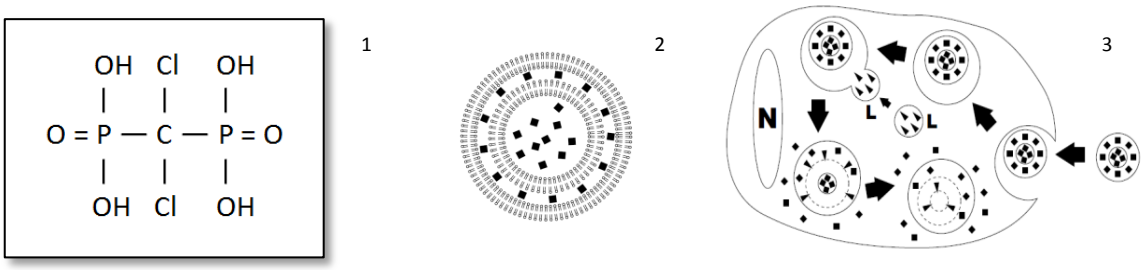

Figure 18. Clodronate structure and mechanism

Clodronate (1) is enclosed in liposomes (2) thus can easily pass the cellular membrane and be phagocytized by macrophages (3). In the cell, liposomes fuse with lysosomes (L) where phospholipases dissolve the lipid shell of liposomes, releasing clodronate in the cytoplasm (N, nucleus).

Rag-$2^{-/-}$ $\gamma_c^{-/-}$ mice were either mock-treated or injected with clodronate liposomes (4 animals treated with clodronate and 4 untreated) before subcutaneous injection with Hey3Met2 control cells in the left flank and RNASET2-expressing Hey3Met2 cells (either wild type or mutant) in the right flank.

In all untreated mice, *in vivo* tumor growth kinetics was very similar to that previously reported in the trial experiment, with a large tumor mass developing in the flank injected with control Hey3Met2 cells when compared to the small-sized tumors of RNASET2-overexpressing Hey3Met2 cells. By contrast, the tumor suppressing activity of wild type RNASET2 turned out to be largely impaired in clodronate treated mice (figure 19).

Unfortunately, xenografts from mice injected with Hey3Met2-overxpressing RNASET2 mutant proved uninformative, since clodronate treatment was ineffective in successfully depleting host macrophages.

UNTREATED MICE

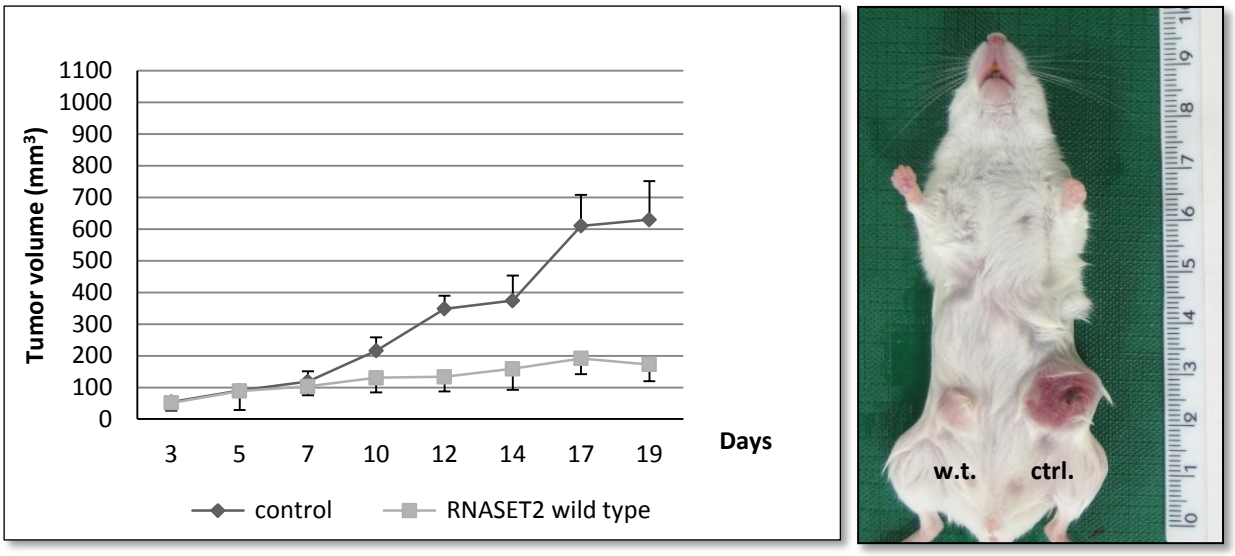

CLODRONATE TREATED MICE

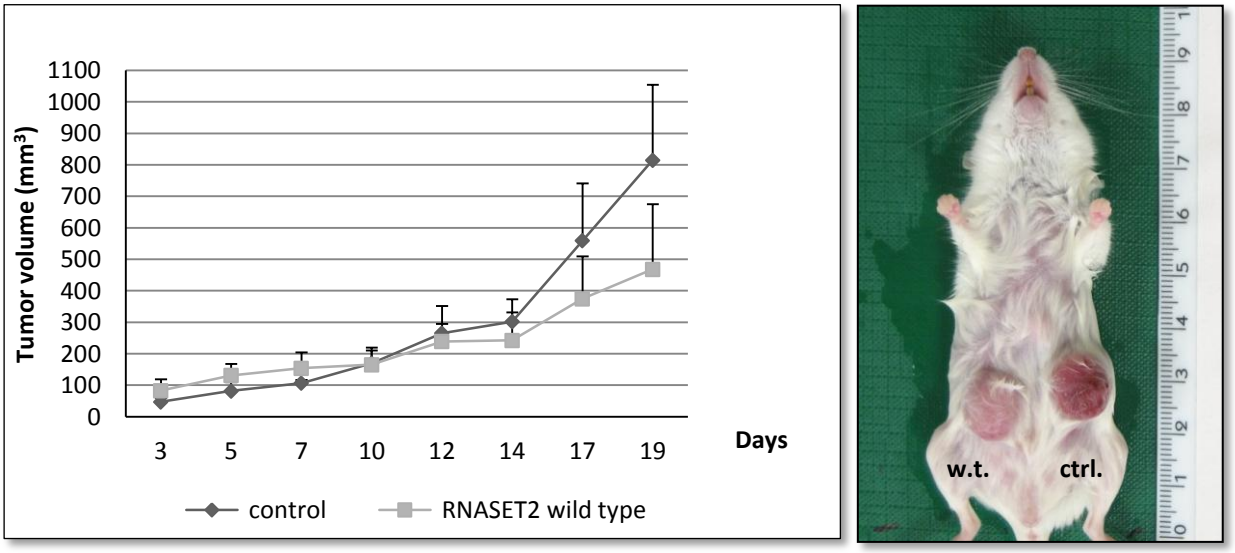

Figure 19. Depletion of macrophages in Rag-2$^{-/-}$ $\gamma_c^{-/-}$ mice

Upper picture. Untreated mice were grafted in the left flank with Hey3Met2 control cells, carrying the pcDNA3 vector, whereas in the right flank Hey3Met2-overexpressing RNASET2 were injected. A considerably reduction of tumor mass is notable.

Lower picture. Mice treated with the macrophage-depleting agent clodronate were grafted as before. RNASET2 wild type resulted strongly impaired in tumor suppression.

Each group of transplanted animals (4 mice/group) was either macrophages depleted or mock treated in both flanks by subcutaneous injection of clodronate liposomes or vehicle alone (PBS) every 6 days, starting at day 2 of the tumor challenge. Animals were monitored twice a week for weight and tumor growth, and sacrificed when the mean tumor volume of one of the subcutaneous tumors reached a dimension of ≥ 800 mm^3.

Bars represent standard deviation values.

At the end of observation period, mice were sacrificed and immunohistochemical characterization of the host cell infiltrate in tumor samples was performed. As shown in figure 20 (right panel), the lack of cells stained with the macrophage-specific marker CD68 confirmed the efficient depletion of macrophages in clodronate-treated mice, whereas these cells could be clearly detected in untreated animal injected with wild-type RNASET2-expressing cells (figure 20, left panel). Tissue macrophages are known to be endowed with a wide functional plasticity, which allows them to carry out both pro-tumoral and anti-tumoral activities depending on microenvironmental cues (56). Therefore, we investigated the pattern of macrophage polarization within RNASET2-expressing tumor xenografts by carrying out IHC assays with markers known to discriminate the differentiation pattern of macrophages into either M1 and M2 subtypes. Interestingly, most of the infiltrating macrophages were of the M1, iNOS-positive type, in keeping with the suggested role of this macrophage subpopulation in tumor suppression (57). These data further support the crucial role for macrophage recruitment in RNASET2-mediated tumor suppression.

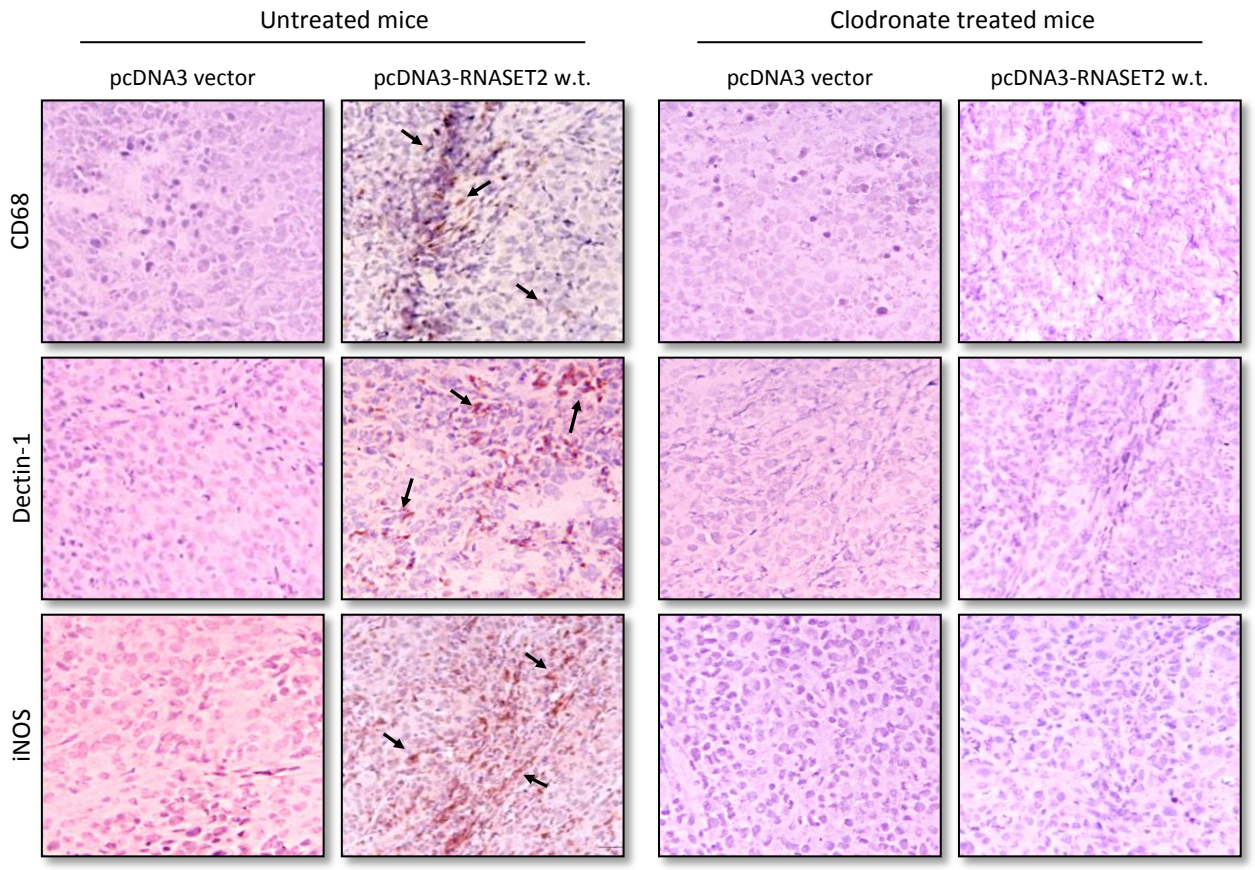

Figure 20. Immunohistochemical characterization of the host cell infiltrate in tumor samples from mock- or clodronate-treated mice. To evaluate the effectiveness of clodronate treatment, tumor sections from Rag-2$^{-/-}$ $\gamma_c^{-/-}$ mice inoculated with control or RNASET2-expressing Hey3Met2 clones were analyses by IHC with the macrophage lineage-specific anti-CD68 glycoprotein antibody. The relative proportion of both M1 and M2 macrophage subpopulations in the tumours was also investigated by means of IHC with anti-iNOS (inducible Nitric Oxide Synthase) and anti-Dectin-1 (surface receptor) antibodies, respectively. Original magnification 40X.

3.4 Knockdown of RNASET2

Based on the data collected with the Hey3Met2 cell line, RNASET2 apparently behaves as a strong suppressor of ovarian cancer development. Thus, it is reasonable to assume that inactivation of this gene (either at the transcriptional level or by a mutational event within coding region of the gene) might represent a critical step in ovarian cancer progression.

To further validate this hypothesis, ovarian cancer cell lines endowed with a low *in vivo* tumorigenic potential and expressing high endogenous RNASET2 levels might provide an ideal experimental model. Since the human ovarian cancer cell line OVCAR3 have the above mentioned features (50, 58), RNAi-mediated silencing has been attempted in this cell line in order to validate the tumor suppressive role of RNASET2 in a second independent model.

RNASET2-specific interfering and scrambled control sequences were defined *in silico* as described in material and methods and subsequently cloned in the lentiviral-derived pSicoR vector. Cultured OVCAR3 cells were then infected with recombinant lentiviral particles, yielding a stable and high efficiently silenced cell line, named OVCAR3::pSicoR-shRNASET2. In control cells, infected with the construct pSicoR-scrambled, the transcription of a mock interfering siRNA occurs but is predicted to leave RNASET2 expression unaffected. Indeed, western blot analysis of total cell extracts with an anti-RNASET2 antibody confirmed the successful silencing of RNASET2 by RNAi (figure 21).

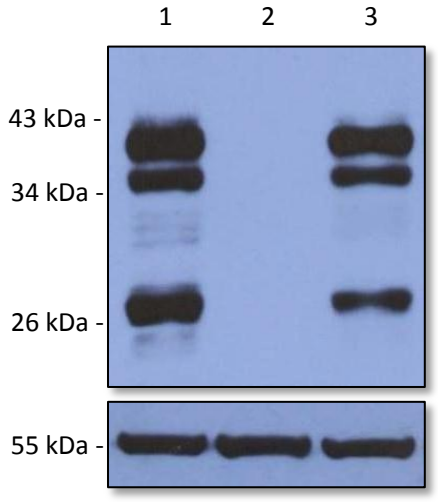

Figure 21. Characterization of RNASET2 knockdown by immunoblot
Upper panel: intracellular lysates of OVCAR3 parental cell line (1), OVCAR3::pSicoR-shRNASET2 (2), OVCAR3::pSicoR-scrambled (3) detected with anti-RNASET2 polyclonal antibody.
Lower panel: the same blot was probed with anti-α-tubulin monoclonal antibody for normalization.

RNASET2-silenced and control clones were then isolated from cellular heterogeneous pools and they are currently under investigation in a wide panel of *in vitro* and *in vivo* assays.

Up to date, growth curve and clonogenic assay have already been completed and showed no differences between RNASET2-silenced and control clones (figures 22 and 23).

These preliminary data are in keeping with the previously described for Hey3Met2 RNASET2-overexpressing model, and further demonstrate the non-cell autonomous behavior of RNASET2 as a tumor suppressor in ovarian cancer models.

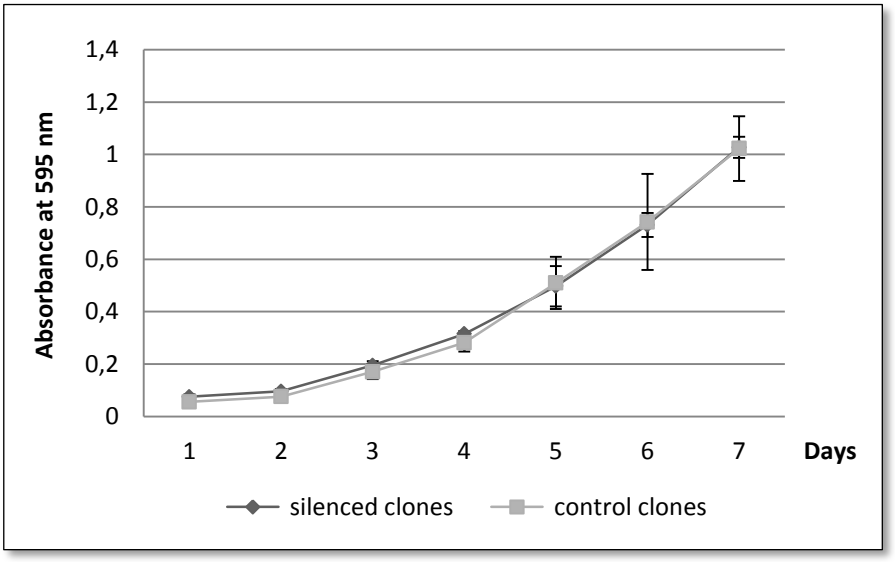

Figure 22. MTT proliferation assay

Three independent clones of both OVCAR3::pSicoR-shRNASET2 and OVCAR3::pSicoR-scrambled are assayed for proliferation. 800 cells per clone are plated in 96-multiwell culture plate in triplicate and growth is monitored for 7 days, sampling cells daily and measuring proliferation spectrophotometrically. Bars indicate the standard deviation values.

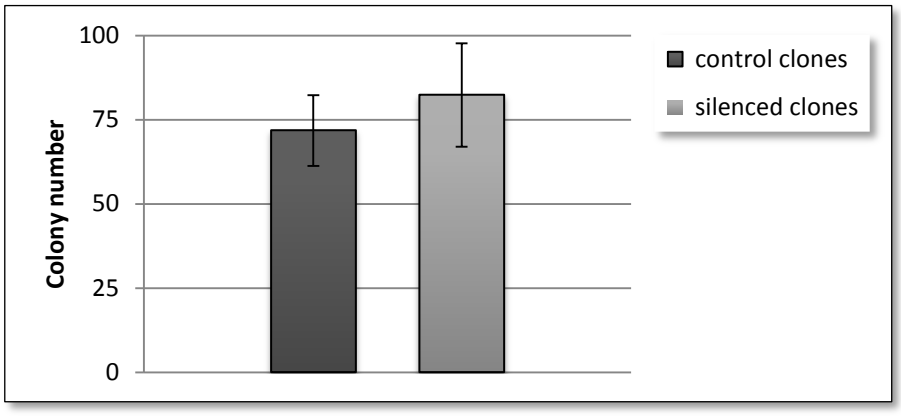

Figure 23. Clonogenic assay

Cells were plated in 6-well culture plates ($1x10^2$ cells per well) and following 14 days incubation, clones were stained with a methylene blue solution (1% methylene blue, 50% ethanol) and visible colonies were manually counted.

The graph is the mean of colonies of three clones per group, each plated in duplicate. Bars indicate the standard deviation values.

Moreover, besides their use in validating the tumor suppressing activity for this gene, RNASET2-silenced OVCAR3 cells also provide an excellent experimental model to start investigating both the intracellular routing of RNASET2 and the mechanism(s) by which extracellular RNASET2 affects cell behavior. Indeed, on the basis of the "asymmetric" behavior observed by comparing the *in vitro* and *in vivo* properties, RNASET2 could be hypothesized to act as a chemokine *in vivo* either directly, by interacting with host immune cells, or indirectly, by triggering the production and secretion of inflammatory chemokines by the cancer cell itself. Under both assumptions, RNASET2 binding to the surface of a target cell would represent a critical step. Moreover, such putative binding to the cell surface could be followed by the internalization of bound RNASET2 within the target cell. Alternatively, RNASET2 could act as a strictly extracellular ligand and trigger an intracellular cascade without being internalized.

To try to shed light on cell surface binding and trafficking, an immunogold localization assay has been performed on silenced OVCAR3 cells exposed to exogenous RNASET2.

As shown in figure 23, whereas no RNASET2 signal could be detected in silenced OVCAR3 cells by transmission electron microscopy (T.E.M.) analysis, a complex localization pattern was found in the same cells treated with exogenous RNASET2 (figure 24).

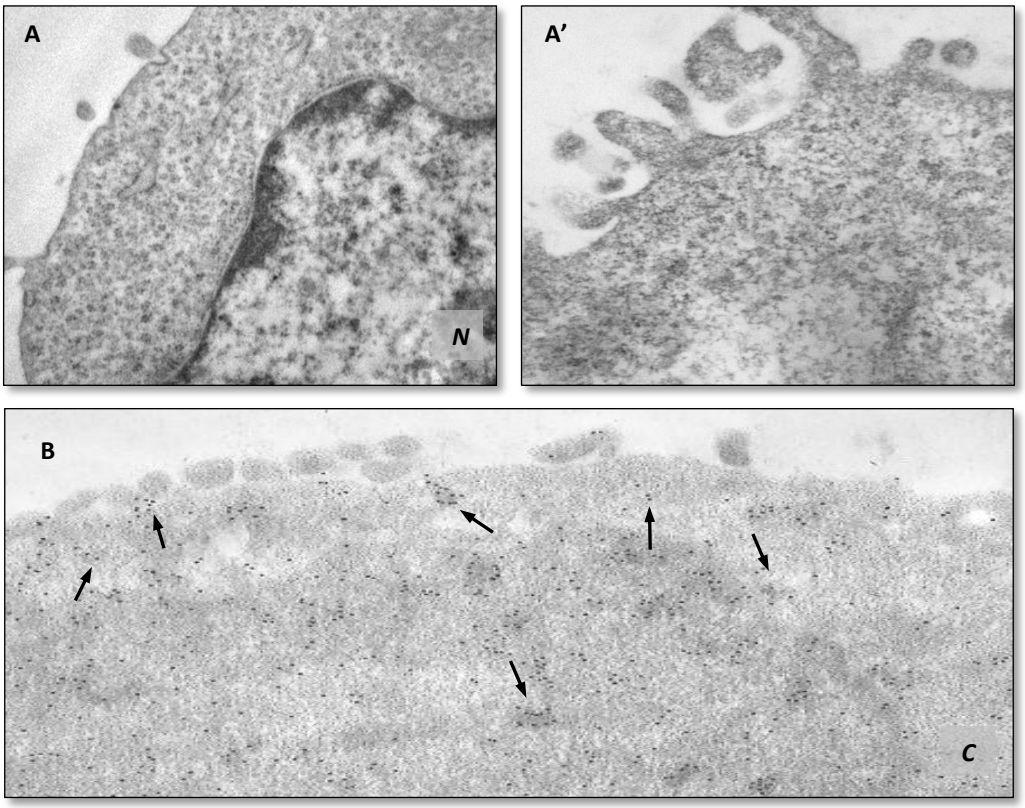

Figure 23. T.E.M. of silenced and parental OVCAR3 cells probed with polyclonal anti-RNASET2

In silenced cells (A – A') no signal is detected, whereas in parental OVCAR3 cells (B) a diffuse RNASET2 signal occurs. *N* – Nucleus, *C* – Cytoplasm.

Exposing OVCAR3 silenced cells to conditioned medium of parental cells (enriched in secreted RNASET2) resulted in binding of the protein to cell surface, thus suggesting the occurrence of a cell surface ligand for this enzyme in OVCAR3 cells (figure 24). Moreover, internalization of RNASET2 was also demonstrated thus suggesting that binding to the cell surface might represent a limiting step for subsequent RNASET2 uptake. If confirmed by further experiment, these preliminary data might also unveil previously unexpected cell-autonomous mechanisms by which RNASET2 might affect cancer cell behavior *via* an autocrine trafficking.

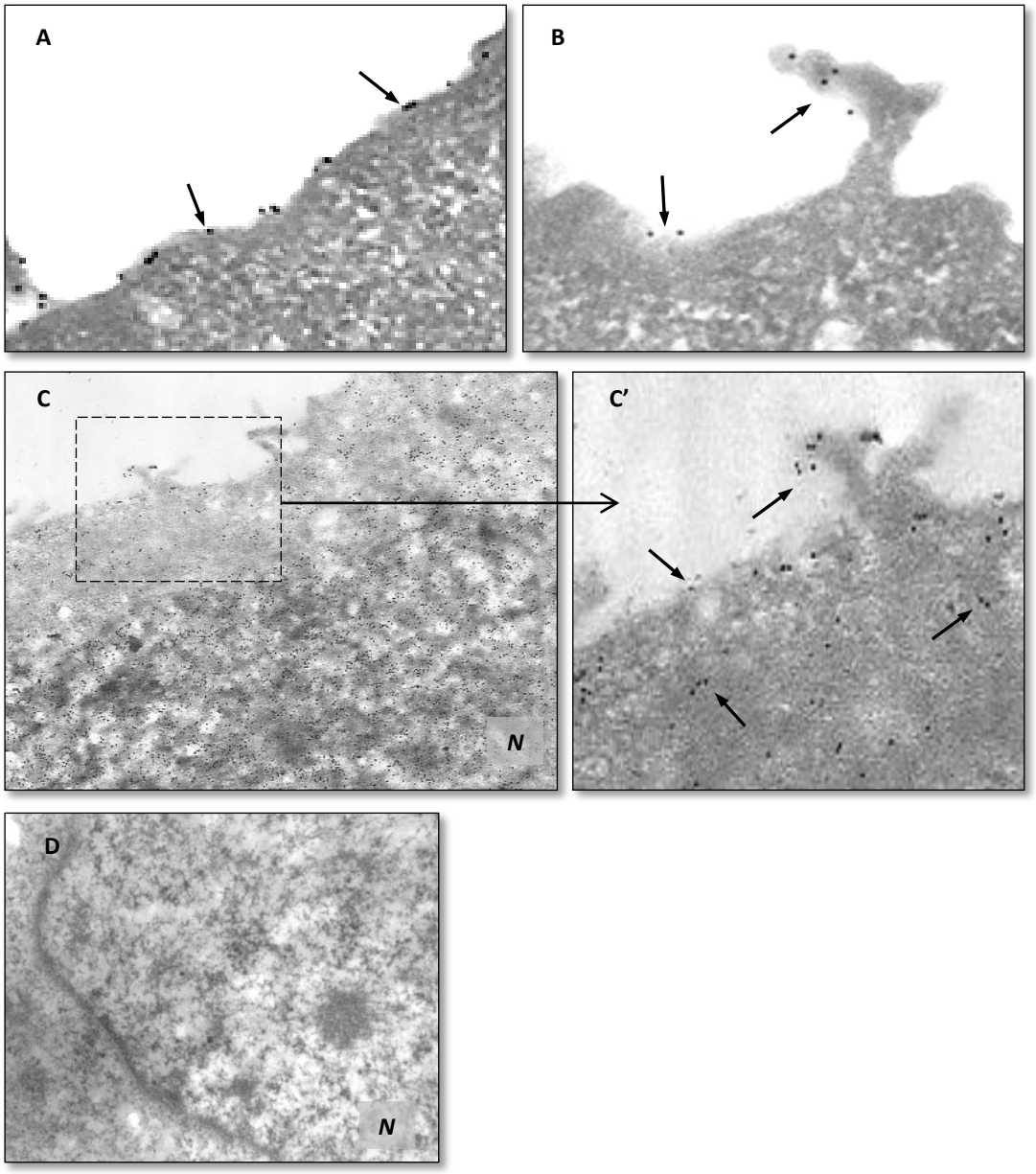

Figure 24. Membrane binding and internalization

Exposing silenced OVCAR3 cells to conditioned medium resulted in an uptake of exogenous RNASET2.

In A and B images a detail of membrane binding is appreciable. In C a widespread signal occurs, indicating the internalization of the protein (particular in C'). In the negative control (D), primary antibody was omitted. *N* – Nucleus.

Furthermore, a detailed inspection of the photomicrographs revealed not only an intracellular localization pattern within vesicles, but strikingly a nuclear signal was also detected (figure 25). Again, this result opens new perspectives on putative pleiotropic roles played by this versatile enzyme.

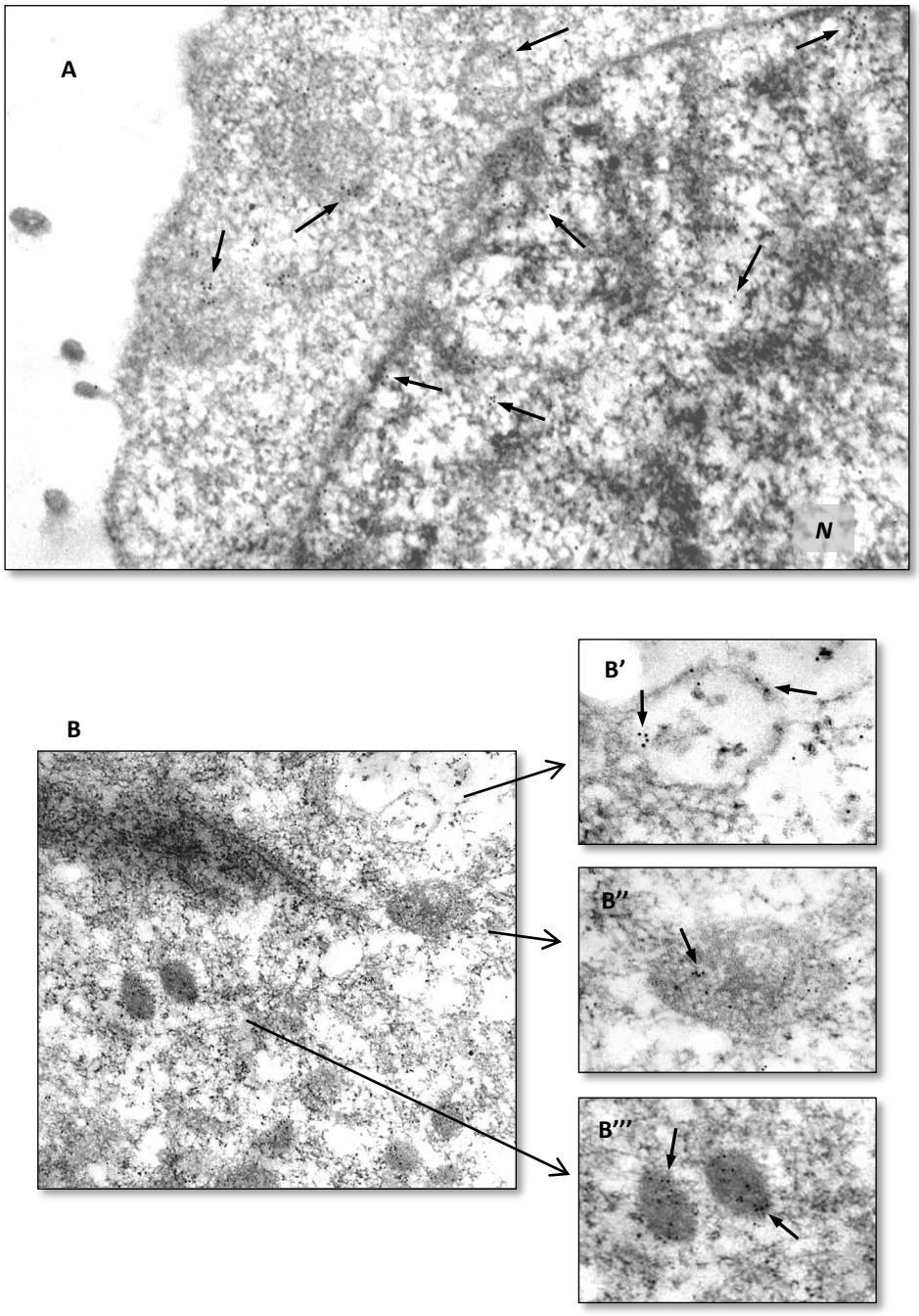

Figure 25. Subcellular localization

Immunogold staining revealed a localization within vesicles (appreciable in A and B') and electron dense structures (B" and B"'). Moreover, an unexpected nuclear localization has been detected. *N* – Nucleus.

4. Discussion

Abnormalities of the long arm of chromosome 6 are associated with several solid neoplasms and hematological malignancies (38-43). Given the broad spectrum of tumours associated with genetic alteration of this genomic region, it has been postulated that the latter could bear tumor suppressor genes playing a general role in tumorigenesis (38). Among the regions of chromosome 6q frequently deleted in tumours, 6q21 and 6q27 have been the focus of intensive investigations in recent years. In the latter region, our group mapped the RNASET2 gene, which represents the first human member of the Rh/T2/S family of ribonucleases.

This gene was shown to be ubiquitously expressed in normal tissues, although at variable levels, but was found to be down-regulated at the RNA level in several ovarian primary tumours and cell lines and in lymphoid neoplasms. Together with its localization in 6q27, these evidences suggested a role for RNASET2 in tumor suppression (50).

In a further functional analysis, our group reported a direct evidence for RNASET2-mediated control of tumor growth *in vivo*. In this study, the low-expressing Hey3Met2 human ovarian cancer cell line was stably transfected with RNASET2 cDNA, and inoculation of transfected clones into athymic mice resulted in a clear inhibition of tumor development. Interestingly, an RNASET2 mutant lacking catalytic activity also showed a similar or even more increased inhibition of tumorigenesis when compared to the wild type protein, suggesting that ribonuclease activity is not involved in control of tumor suppression and metastasis (51). The more efficient tumour suppressor activity of the mutant form was an intriguing finding that still has to be cleared. Although this observation could be simply explained by a slight difference in the expression levels in mutant compared to wild type RNASET2-expressing clones (assuming that both protein forms display the same tumor suppressive activity), we cannot rule out more complex mechanisms. Therefore, this issue will likely be definitively solved when further structural and functional investigations of both wild type and mutant RNASET2 will be performed. However, it is worth noting that a catalytically independent biological role has also been reported for other members of the T2 family (33).

The finding of a tumor suppressing ribonuclease is not unexpected, since an oncosuppressive role has already been demonstrated for other genes encoding for this class of enzymes. For example, human ribonuclease L (RNase L), which maps to 1q25, has been linked to susceptibility to hereditary prostate cancer (HPC1), and some its variants were associated with aggressive metastatic prostate neoplasia (59, 60).

Moreover, many examples of cytotoxic ribonucleases endowed with anticancer activity belonging to A family have been reported. The most representative are BS-RNase and Onconase, known to be highly cytotoxic to cancer cells. The former has been shown to possess anticancer activity against several tumor

types, including thyroid carcinoma and neuroblastoma cells (17-20), whereas the latter is currently under phase III clinical trials for unresectable malignant mesothelioma (14).
Significantly, a strong antitumor activity has also been described for a fungal member of T2 family ribonucleases, namely ACTIBIND. Unrelated to its RNase activity, ACTIBIND binds actin filaments *in vitro*, resulting in altered actin organization and cell morphology. This is in turn reflected in reduced *in vitro* colony formation and motility of several tumor cell lines. *In vivo*, ACTIBIND inhibits growth and metastasis in colon cancer and melanoma mouse model (36, 37) and inhibits angiogenesis both *in vitro* and *in vivo* by directly competing with angiogenin.

With the aim to further understanding the mechanisms at the basis of tumor suppressor activity mediated by RNASET2, a comparative analysis by means *in vitro* and *in vivo* assays has been carried out in this work.
Thus, in order to verify if RNASET2 could control tumor development at cellular level (*i.e*. in a cell-autonomous manner), several *in vitro* test were carried out with Hey3Met2 RNASET2-overexpressing clones. By comparing several parameters such as cell proliferation, apoptosis, clonogenicity and growth on semisolid media, it was found that RNASET2 had no effect on these cellular features *in vitro*. Noteworthy, at least for proliferation and clonogenic assay, the same results was obtained in the OVCAR3 knockdown RNASET2 model, further supporting the hypothesis of a non-cell autonomous behavior.
On the other hand, when the same Hey3Met2 clones were investigated *in vivo* we could easily confirm the previous evidence of a strong oncosuppressive activity carried out by this gene.
This sharp difference of RNASET2 behavior between the two experimental models was not completely unexpected, since other tumor suppressor genes have been reported to display such "asymmetric" behavior *in vitro/in vivo* in the control of malignancy (11, 12). Indeed, based on this particular feature a new class of tumor suppressor genes has been recently proposed, namely the tumor antagonizing- or malignancy suppressor-genes (TAGs/MSGs) (2). These genes are functionally defined by having no effect on tumor growth *in vitro,* whereas their function is clearly detected *in vivo* and is likely mediated by the establishment of a cross-talk between the cancer cell and the tumor microenvironment (3, 4, 5).
Among tumor antagonizing genes, worth mentioning are the hyaluronidase HYAL1 and HYAL2 genes and the WWOX gene.
HYAL1 and HYAL2 are located in the minimal region of homozygous deletion for lung cancer (LUCA) in the 3p21 region and encode for enzymes involved in the catabolism of hyaluronic acid. Inactivation of one of the two genes lead to accumulation of hyaluronan in the extracellular compartment, which in turn enhances anchorage independent tumor cell growth (11). Since the product of both genes have a potential to influence intercellular interactions, their impairment inhibit microenvironmental control mechanisms that normally protect the host from tumor growth.

As far as the WWOX gene is concerned, restoration of its expression in human PE01 ovarian cancer cells causes reduction of tumor development in SCID mice *in vivo* but not *in vitro* (12). By altering the levels of membrane-associated integrin α_3, WWOX-overexpressing cells show reduced adhesion to the extracellular matrix component fibronectin that in turn is reflected in a reduced survival rate *in vivo*.

Current cancer research is increasingly focusing on the study of tumour microenvironment, which is the complex system of cells and extracellular matrix surrounding the malignant milieu. Several recent reports suggest that carcinogenesis should be regarded as phenomena occurring in tissues and not just in individual cancer cells (6-10). Indeed, the tumour microenvironment is known to strongly influence the propensity of neoplastic cells to proliferate *in vivo*, either through direct contact between tumour and stromal cells or by means of soluble ligands interacting with cell receptors. More specifically, the genes whose products might participate in the regulation of tumour interaction with stromal cells and extracellular matrix are predicted to be involved in three types of processes: 1) response to differentiation-inducing signals *in vivo*; 2) response to microenvironmental signals; 3) angiogenesis inhibition (4).

Strikingly, the detailed histochemical examination of tumour sections isolated from athymic mice inoculated with RNASET2-transfected ovarian cancer cells showed a completely different tissue architecture with respect to controls, pointing out a remodeling of surrounding stromal environment exerted by RNASET2. Particularly interesting was the finding of a massive infiltrate of host cells, with abundant deposition of connective tissue and collagen fibers in RNASET2-overexpressing tumors.

Morphological and histochemical analyses indicated this host cellular population infiltrating the neoplastic mass was made of cells belonging to monocyte/macrophages lineage.

The macrophage represent a rather versatile cell type displaying pleiotropic biological roles which includes antigen presentation, target cell cytotoxicity, removal of debris and tissue remodeling, regulation of inflammation, induction of immunity, thrombosis and various forms of endocytosis (56).

In the frame of tumour development, tumour-associated macrophages (TAMs) have a wide range of functions which could affect diverse aspects of neoplastic growth such as angiogenesis, matrix deposition and remodeling, modulation of tumor cell growth (both enhancement and inhibition) and neoplastic cell death (cytotoxicity, apoptosis) (57, 61).

In this conceptual framework, we turned our attention to the putative mechanisms underlying RNASET2-mediated tumor suppression. To this aim, three main processes were investigated such as proliferation rate, apoptosis and vascularization. Whereas the latter seemed to be similar in all analyzed specimens, a decreased proliferation rate in addiction to markedly cell death was observed in RNASET2-transfected tumors, suggesting that the synergistic effect of these two parameters could be at the basis of the strong decrease of tumor mass observed.

The functional role of macrophages infiltration in the control of tumorigenicity was also directly confirmed by means of a new xenograft assay in Rag-$2^{-/-}$ $\gamma_c^{-/-}$ mouse model.

Indeed, in macrophage-depleted mice the tumor growth kinetics of control and RNASET2-expressing cells were very similar, whereas in untreated mice large tumor masses developed in the flank injected with control Hey3Met2 cells compared to the small-sized tumors of RNASET2-overexpressing Hey3Met2 cells, as previously reported.

A further investigation on the infiltrating macrophage polarization pattern was also carried out in our $Rag2^{-/-}\gamma_c^{-/-}$ mouse model.

Indeed, by expressing different functional programs in response to particular conditions present within the tumour microenvironment (62) macrophages possess activities that can either prevent the establishment and spread of tumor cells or support tumor progression and metastatization. This ambivalent relationship between macrophages function and cancer is due to the high functional plasticity of these cells that has been mentioned before.

Such different polarization of TAMs is also referred as M1-"classical activated" *vs.* M2-" alternatively activated" phenotype, indicating the anti-tumoral and pro-tumoral properties respectively.

"Classical activated" M1 type macrophages participate to the innate host defense against pathogens. They are stimulated by microbial agents, interferon-γ and TNF-α and are generally considered potent effector cells against microorganisms and tumor cells by means of pro-inflammatory cytokines secretion, in addition to a high production of toxic products such as nitric oxide (NO) and reactive oxygen intermediates (ROI). Alternatively, activated macrophages (M2) are normally involved in wound healing, where they participate in tissue remodeling and secretion of growth factors that stimulate fibroblast proliferation, migration, and extracellular matrix formation. Nevertheless, in the context of a growing tumor and under different stimuli such as hypoxia and several inducers (such as cytokines IL-10, IL-4 and glucocorticoid hormones), M2 macrophages can promote tumor growth by producing growth factors that enhance cancer proliferation (such as PDGF and EGF), dissemination (metalloproteinases) and angiogenesis via VEGF production (63).

In RNASET2-expressing tumors both M1 iNOS (inducible Nitric Oxide Synthase) positive macrophages and M2-dectin1 positive macrophages were found, with a prevalence of M1 cells, in keeping with the anti-tumor activity owned by these cells. The presence of M2 type could be explained by virtue of the high functional plasticity of macrophages which are able to finely modulate their programs in response to different microenvironmental conditions. Indeed, dynamic changes of the tumor microenvironment that occur during the transition from early neoplastic events toward advanced tumor stages (such as hypoxia, glucose levels, pH and tumor cells products including extracellular matrix components, IL-10 and CSF-1 (Colony Stimulating Factor 1) that are thought to occur, drive an M1-to-M2 switch (63).

Taken together, our data suggest that RNASET2 most likely could act as a tumor antagonizing gene, by playing an inflammatory-like role.

Significantly, functional interactions between enzymes endowed with RNase activity and immune system cells is not unexpected. As an example, alarmins are defined as endogenous mediators rapidly released by cells of the host innate immune system in response to infection and/or tissue injury, which possess the

dual activity of recruiting and activating dendritic cells and consequently enhance antigen-specific adaptive immune responses.

Mammalian eosinophil granules contain an antimicrobial protein known as eosinophil-derived neurotoxin (EDN), which belongs to the RNase A superfamily and has antiviral and chemotactic activities, inducing migration and maturation of dendritic cells. The latter enhance the adaptive immune system response by stimulating lymphocytes T helper maturation (Th2 polarization) (64, 65).

Another connection between RNases and immune system arises from a T2 ribonuclease present in the eggs of the worm *Schistosoma mansoni*, a trematode parasitic of human beings. Eggs secrete a glycoprotein termed omega-1, which is a member of RNaseT2 family. Recent data (66) showed that both *in vitro* and *in vivo* omega-1 is the major component in priming dendritic cells for Th2 polarization of CD4+ T cells during infection. However, this function appears to depend on the RNase activity of omega-1, as inactivation of the ribonuclease activity inhibits the Th2-polarizing function (67).

The assumption that RNASET2 could act as a signaling molecule is also supported by preliminary immunolocalization studies carried out with OVCAR3 silenced cells. In this view, two main possible scenarios can be proposed. In the first, RNASET2 would act as a chemokine-like ligand, binding directly the host immune cells to trigger an intracellular response; in the second scenario, RNASET2 would elicit the production of an inflammatory chemokine(s) by the cancer cell itself. By exposing RNASET2-silenced ovarian cancer cells to conditioned medium enriched in exogenous RNASET2, we could observe both the binding of the protein to cell surface and its subsequent internalization, two critical steps involved in cell-ligand interactions.

Although this assay opens up the possibility of an autocrine trafficking of RNASET2 and thus supports the second hypothesis, we cannot rule out the possibility that RNASET2 could also act as a signaling molecule by itself, and further studies (e.g. monocytes chemoattractant assay with recombinant protein) will be carried out to investigate this issue.

Finally, the putative autocrine pathway observed in cancer cells raised the question whether RNASET2 could have an additional cell-autonomous activity.

Recent works (35, 68) have reported that during oxidative stress the yeast RNASET2 orthologue Rny1p is released from the vacuole to the cytoplasm, where it cleaves cytoplasmic tRNAs and rRNAs. Moreover, Rny1p also modulates yeast cell survival during oxidative stress, resulting in reduced cell viability and apoptosis, and this effect is carried out independently of its catalytic activity, arguing that Rny1 has a second function involving promotion of cell death, unrelated to its ability to cleave RNA. Interestingly, by means functional complementation, RNASET2 was found to restore tRNA cleavage and confer a similar loss of viability and apoptosis susceptibility under stress conditions as the endogenous protein. Hence, the apoptotic phenotype triggered *in vivo* by RNASET2 might be ascribed not only to macrophage recruitment and activation but perhaps to RNASET2 cell-autonomous effects within tumor cells as well, as observed in yeast cells.

5. Materials and methods

Cell cultures, transfections and infections

The Hey3Met2 and OVCAR3 human ovarian cancer cell lines were maintained in DMEM-F12 medium, supplemented with 10% FBS and 2 mM L-glutamine (Gibco) and grown at 37 °C in a 5% CO_2 atmosphere.

For transfection experiments, Hey3Met2 cells were plated in 6-well plates the day before experiment, to reach 80% confluence at transfection, which was performed with Lipofectamine 2000 (Invitrogen), according to the manufacturer's instructions. Forty-eight hours after transfection, cells were trypsinized and transferred into 100 mm cell culture plates and selected with 300µg/ml G418 (Invitrogen). After two weeks, single transfected clones were isolated using cloning rings. A western blot analysis was carried out with a rabbit polyclonal anti-RNASET2 antibody (1:1000) on total protein extract (30 µg/lane) from each clone, to evaluate the level of RNASET2 expression. Clones displaying the highest RNASET2 expression levels were selected for experiments.

For infection experiments, packaging cell line HEK 293T were transfected with pSicoR-shRNASET2 or control construct pSicoR-scrambled in addiction to viral components (GAG-POL, ENV). The day after transfection, HEK 293T cells supernatant is collected, filtered with 0.45µm pore filter and used to infect OVCAR3 cells. Forty-eight hours after infection cells are selected with 1.5µg/ml puromycin (Sigma). Cell cultures were routinely checked for the presence of contaminating mycoplasma by a nested PCR method described in Tang *et al*. (69).

In vitro cell based assays

Growth curve

In vitro cell growth curves were assembled by plating 4000 cells in a 24-well culture plate and counting viable cells daily in triplicate on a Burker chamber for 8 days. Growth curve is obtained plotting the log of cell number against time.

Doubling time is determined using the formula $T_c = (0.3T)/\log (A/A_0)$, where "A" is the number of cells counted at "T" time, and "A_0" is the initial number of seeded cells. Values of "T" and "A" are considered in the portion of semi-log plot where the shape of the curve is a straight line.

BrdU incorporation and apoptosis

For BrdU incorporation assay, Hey3Met2 cells were plated on coverslips in 6-well plates until they reached 70% confluence and are in logarithmic phase of cell division. Subsequently are pulsed with a 10µM solution of BrdU for 1 hour and according to BrdU in-Situ Detection Kit (BD) are fixed, permeabilized and labeled with biotinylated anti-BrdU antibody 1:10, followed by streptavidin-HRP conjugated incubation. Immunostaining is then performed with diaminobenzidine (DAB) as substrate. For negative controls, BrdU antibody was omitted.

For apoptosis detection cells are plated as before and fixed in 4% paraformaldehyde. According to DeadEnd™ colorimetric TUNEL (Promega) cells are permeabilized and incubate with biotinylated buffer mix enzyme containing TdT polymerase and nucleotides at 37°C for 60 minutes. Immunostaining is then performed with DAB as substrate. For negative controls, Terminal Deoxynucleotidyl Transferase Recombinant (rTdT) was omitted.

Clonogenic assay, soft agar growth and adhesion test

To carry out colony formation assay, cells were plated in 6-well culture plates (2 x 10^2 cells per well). Following a 10-14 days incubation, clones were stained with methylene blue solution (1% methylene blue w/v, 50% ethanol) and visible colonies were manually counted. Each clone was assayed in triplicate.

In order to estimate colony formation in anchorage independent manner, two-layers soft agar test was performed. For each clone 100 cells are resuspended in an upper layer of 0.3% Bacto-Agar in DMEM F12 and 20% fetal bovine serum and then plated over an under layer of 0.6% Bacto-Agar in DMEM F12 and 20% fetal bovine serum in a 12 well culture plate. Each clone was assayed in triplicate and colonies after 14 days were counted.

Adhesion test has been carried out plating Hey3Met2 clones onto 96-well matrigel coated (50µg/ml, Sigma) ($5x10^3$ cells/clone, 10 wells/clone). Four hours after seeding cells, growth media is removed and cells are fixed/stained with 37% formaldehyde and 0.75% (w/v) crystal violet solution. After several washes, dye is eluted in 50% ethanol, 0.1% acetic acid solution and absorbance at 595 nm is measured.

MTT proliferation assay

Silenced and control OVCAR3 clones are seeded in triplicate in 96-well plate ($8x10^2$ cells/well, one plate per day) and growth in monitored for 7 days. According to the manufacturer's instructions (CellTiter 96® Non-Radioactive Cell Proliferation Assay, Promega) 15µl of tetrazolium salt is added to each well and formazan product is detected after 4 hours of incubation, by 96-well plate reader at 595 nm.

In vivo xenograft studies

For tumorigenicity test, 5 athymic male mice per clone or female $Rag2^{-/-}\gamma_c^{-/-}$ (3 animals/clone) were grafted by means subcutaneous injection with $5x10^6$ Hey3Met2 cells (control or Hey3Met2 cells expressing wild-type RNASET2 or RNASET2 mutant), resuspended in 0.15 ml of growth medium and 0.15 ml of matrigel (Sigma). Animals were monitored twice a week for weight and tumor growth (measuring three perpendicular diameters), and sacrificed when the mean tumor volume of control mice reached a dimension of $\geq$1000 mm^3.

Macrophages depletion in $Rag2^{-/-}\gamma_c^{-/-}$ mice was carried out using clodronate liposomes (Roche).

Four animals/clone were injected subcutaneously with control Hey3Met2 cells in the left flank and with Hey3Met2 cells expressing either wild-type or catalytically impaired mutant RNASET2 in the right flank.

Each group of transplanted animals was either macrophage-depleted or not by subcutaneously injection in both flanks of clodronate liposomes (50ml/flank) every 6 days, starting at day -2 of the tumor challenge. Mice were monitored twice a week for weight and tumor growth, and sacrificed when the mean tumor volume reached a dimension of 800 mm^3. Animals were maintained in a pathogen–free facility and treated in accordance with the European guidelines under the approval of the Ethical Committee of the Istituto San Raffaele of Milan.

Histological and immunohistochemical assays

Harvested tumors were either fixed in buffered 4% formalin either embedded in OCT and frozen in liquid nitrogen. 3μm paraffin sections were either stained with hematoxylin and eosin or with Masson's trichrome staining (Sigma) for morphological analysis. Cryosections were immunostained with the with the following primary antibodies after antigen retrieval: anti-RNASET2 (1:100); rabbit anti-cleaved caspase-3 (1:20, Santa Cruz Biotechnology) rat anti-mouse CD11b (1:50, Pharmingen), rat anti-human Ki-67 (1:100, Dako) and rat-anti F4/80 (1:50, Pharmingen). The immunoreactions were revealed either by biotinylated-conjugated anti-rat antibody (Vector), horseradish peroxidase-conjugated streptavidin either by rabbit or rat on rodent HRP-polymer (Biocare Medical) and using DAB as chromogenic substrate (Biogenex). Slides were counterstained with hematoxylin. Photomicrographs were taken using the AxioCam HRc (Zeiss) with the AxioVision System 6.4.

To evaluate blood vessel density in tumor samples, cryosections were treated with 50mM levamisole to block endogenous alkaline phosphatase. A mouse anti-human PECAM-1 (CD31) antibody (1:20, Dako) was then incubated for 1h at 37°C, followed by a 45 min treatment with a secondary goat anti mouse AP-conjugated antibody (1:200). The signal was detected with BCIP/NBT Alkaline Phosphatase Substrate Solution (Sigma). Control reactions were carried out by omitting the primary antibody.

For CISH analysis, the ZytoDot probe kit (Histo-Line) was used to hybridize a biotinylated murine chromosome Y-specific centromeric probe to serial sections of Hey3Met2-derived tumors according to the manufacturer's instructions.

Macrophages populations in clodronate-treated and control animals were detected on cryosections obtained as described above and treated with 0.3% H_2O_2 in PBS to remove endogenous peroxidase. Washed sections were incubated for 1h at 37°C with the following biotinylated primary antibodies: rat anti-mouse CD68 (1:100, HyCult Biotechnology), rat anti-mouse Dectin-1 (1:50 Cell Sciences) and rabbit anti-mouse iNos-2 (1: 10, Santa Cruz Biotechnology). The washed specimens were incubated for 30 min at room temperature with streptavidin-peroxidase (Dako), washed , and signal was detected with 0.05% DAB and 0.03% H_2O in PBS. Sections were counterstained with hematoxylin. Coverslips were mounted and slides were examined with a microscope Olympus.

Electron microscopy

For immunogold cytochemistry, samples were fixed for 2h at 4°C with 4% paraformaldehyde and 0.5% glutaraldehyde in PBS, dehydrated in ethanol series and impregnated in Epon-Araldite 812 mixture. After etching with 3% NaOH in absolute ethanol, ultrathin sections (80nm in thickness) were placed on conventional nickel grids and incubated overnight at 4°C with primary rabbit polyclonal anti-human RNASET2 diluted 1:40 in saturation buffer (1% NGS, 1% ovalbumin in TBS). Primary antibodies were visualized by immunochemical staining with secondary goat anti-rabbit IgG (H+L)-gold conjugate antibodies (GE Healthcare Amersham, Buckingamshire, UK) (particle size 15nm) diluted 1:100 (incubation 2h at room temperature). Control sections were incubated in saturation buffer and then with secondary antibodies alone. Samples were counterstained with 2% uranyl acetate in water and observed under electron microscopy Jeol 1010 EX electron microscope.

Western blot

Total protein extracts were obtained by scraping cells with PBS-EDTA 10mM, and lyse them with 5mM EDTA, 0.5% NP40, 0.5% Triton X-100 in PBS buffer, supplemented with a mixture of protease inhibitors (PMSF, benzamidine, aprotinin, and leupeptin). Quantitation of total protein was performed with Bradford reagent (BioRad), using bovine serum albumin as standard. Intracellular lysates were loaded on a 13% SDS-PAGE (30µg/lane) and then transferred to a nitrocellulose membrane which was blocked in 4% w/v of non-fat milk in PBS-T (0.1% Tween 20 in PBS buffer) and probed with rabbit anti-RNASET2 (1:1000) or mouse anti-α-tubulin (1:1000 Sigma). Immunoblot analysis was then performed according to standard procedures with HRP-conjugated secondary antibodies (anti-rabbit 1:900 and anti-mouse 1:900, Pierce) and detected with the chemiluminescent substrate SuperSignal West Dura (Pierce).

Plasmid vectors and sequences design for RNA interference

Several interfering sequences for RNASET2 gene have been generated with pSicoOligomaker 1.5 program, and were aligned with BLAST algorithm against the whole transcriptome database, in order to choose the only sequence able to target uniquely RNASET2 without alter other transcripts. Scrambled sequence were designed having the same GC% content of the interfering sequence but does not match with any transcript present in database.

Interfering and scrambled oligonucleotides are constituted by a short sequence of 19 nucleotides (directly involved in pairing with RNA, in the box below) inserted within a wider nucleotide context required for correct folding of the transcript, giving rise to the stem-loop structure.

Interfering sequence (sense strand)

5’ TGCAGAAGCCTGGAACTCTATTCAAGAGATAGAGTTCCAGGCTTCTGCTTTTTTC

Scrambled sequence (sense strand)

5’ TGAGTCGACCGAACAGTCTATTCAAGAGATAGACTGTTCGGTCGACTCTTTTTTC

Sense and antisense strands of both oligonucleotides were annealed in appropriate buffer (100 mM potassium acetate, 10mM HEPES-KOH pH 7, 2mM Magnesium acetate), slowly cooling down the temperature from 70°C to 4°C (1°C/min). Annealed oligonucleotides are then cloned in XhoI/HpaI digested pSicoR vector.

pSicoR vector (plasmid for Stable RNA Interference, COnditional Reverse) is a lentiviral-derived vector for stable expression of shRNAs (70) that efficiently drives short hairpin transcription under the control of RNA polymerase III specific-promoter U6. pSicoR vector could be either transfected in target cells or delivered by means infection and Lox-P sites flanking the short hairpin expression cassette allow to remove it by Cre-lox-P mediated recombination.

Statistical analysis

The results from *in vitro* and *in vivo* assays with Hey3Met2 cells were evaluated by means of one-way ANOVA test with fixed p value ≤ 0.05, whereas the Student t-test was used to analyze *in vitro* assays performed with OVCAR3 cells.

6. References

1 Klein G. (1993). *Genes that can antagonize tumor development*. FASEB J. Jul;7(10):821-5

2 Islam MQ and Islam K (2000). *A new functional classification of tumour-suppressing genes and its therapeutic implications*. BioEssays 22(3): 274-85

3 Imreh S, Klein G, Zabarovsky ER. (2003). *Search for unknown tumor-antagonizing genes*. Genes Chromosomes Cancer. Dec;38(4):307-21

4 Klein G, Imreh S, Zabarovsky ER. (2007). *Why do we not all die of cancer at an early age?*. Adv. Cancer Res. 98:1-16

5 Klein G. (2009). *Toward a genetics of cancer resistance*. Proc Natl Acad Sci USA 106:859-863

6 Liotta LA, Kohn EC. (2001). *The microenvironment of the tumour-host interface*. Nature. May 17;411(6835):375-9.

7 Bissell MJ, Radisky D. (2001). *Putting tumours in context*. Nat. Rev. Cancer. Oct;1(1):46-54.

8 Mueller M, Fusenig N. (2004). *Friends or foes - bipolar effects of the tumor stroma in cancer*. Nature Rev. Cancer 4:839-842

9 Nelson CM, Bissell MJ. (2006). *Of extracellular matrix, scaffolds, and signaling: tissue architecture regulates development, homeostasis, and cancer*. Annu Rev Cell Dev Biol. 22:287-309

10 Alphonso A, Alahari SK. (2009). *Stromal cells and integrins: conforming to the needs of the tumor microenvironment*. Neoplasia. Dec;11(12):1264-71

11 Wang F, Grigorieva EV, Li J, Senchenko VN, Pavlova TV, Anedchenko EA, Kudryavtseva AV, Tsimanis A, Angeloni D, Lerman MI, Kashuba VI, Klein G, Zabarovsky ER (2008). *HYAL1 and HYAL2 inhibit tumour growth in vivo but not in vitro*. PLoS One. Aug 22;3(8):e3031

12 Gourley C, Paige AJ, Taylor KJ, Ward C, Kuske B, Zhang J, Sun M, Janczar S, Harrison DJ, Muir M, Smyth JF, Gabra H. (2009). *WWOX gene expression abolishes ovarian cancer tumorigenicity in vivo and decreases attachment to fibronectin via integrin alpha3*. Cancer Res. Jun 1;69(11):4835-42

13 Rosenberg, H.F. (2008). *RNase A ribonucleases and host defense: an evolving story*. J. Leukoc. Biol.83, 1079–1087

14 Porta C, Paglino C, Mutti L., (2008). *Ranpirnase and its potential for the treatment of unresectable malignant mesothelioma*. Biologics. Dec;2(4):601-9

15 Irie M.(1999). *Structure-function relationships of acid ribonucleases: lysosomal, vacuolar, and periplasmic enzymes*. Pharmacology & therapeutics. 81 :77-89

16 Ilinskaya ON, Zelenikhin PV, Petrushanko IY, Mitkevich VA, Prassolov VS, Makarov AA. (2007). *Binase induces apoptosis of transformed myeloid cells and does not induce T-cell immune response*. Biochem Biophys Res Commun. Oct 5;361(4):1000-5

17 Lee I, Lee YH, Mikulski SM, Lee J, Covone K, Shogen K. (2000) *Tumoricidal effects of onconase on various tumors*. J Surg Oncol. Mar;73(3):164-71

18 D. Spalletti-Cernia, R. Sorrentino, S. Di Gaetano, A. Arciello, C. Garbi, R. Piccoli, G. D'Alessio, G. Vecchio, P. Laccetti, M. Santoro.(2003). *Antineoplastic ribonucleases selectively kill thyroid carcinoma cells via caspase-mediated induction of apoptosis*. J. Clin. Endocrinol. Metab. 88; 2900–2907

19 A. Antignani, M. Naddeo, M.V. Cubellis, A. Russo, G. D'Alessio. (2001). *Antitumor action of seminal ribonuclease, its dimeric structure, and its resistance to the cytosolic ribonuclease inhibitor*. *Biochemistry* 40; 3492–3496

20 I. Marinov, J. Soucek. (2000). *Bovine seminal ribonuclease induces in vitro concentration dependent apoptosis in stimulated human lymphocytes and cells from human tumor cell lines*. Neoplasma 47; 294–298

21 A. Bracale, D. Spalletti-Cernia, M. Mastronicola, F. Castaldi, R. Mannucci, L. Nitsch and G. D'Alessio. (2002). *Essential stations in the intracellular pathway of cytotoxic bovine seminal ribonuclease*. Biochem. J. 362; 553–560

22 Mastronicola MR, Piccoli R, D'Alessio G. (1995). *Key extracellular and intracellular steps in the antitumor action of seminal ribonuclease*. Eur J Biochem. 230:242–249

23 Darzynkiewicz, Z., Carter, S.P., Mikulski, S.M., Ardelt, W., Shogen, K. (1988) *Cytostatic and cytotoxic effects of Pannon (P-30 Protein), a novel anticancer agent*. Cell Tissue Kinet. 21, 169–182

24 Mikulski, S. M., Ardelt, W., Shogen, K., Bernstein, E. H. and Menduke, H. (1990). *Striking increase of survival of mice bearing M109 Madison carcinoma treated with a novel protein from amphibian embryos*. J. Natl. Cancer Inst. 82, 151-153

25 M. Rybak, D.L. Newton. (1999). *Natural and engineered cytotoxic ribonucleases: therapeutic potential*. Exp. Cell Res. 253; 325-335

26 Márquez,M., Nilsson, S., Lennartsson, L., Liu, Z., Tammela, T., Raitanen, M., Holmberg, A.R. (2004). *Charge-dependent targeting: results in six tumor cell lines*. Anticancer Res. 24, 1347–1351

27 Ardelt, B., Ardelt, W., Darzynkiewicz, Z. (2003). *Cytotoxic ribonucleases and RNA interference*. Cell Cycle 2, 22–24

28 Zhao H, Ardelt B, Ardelt W, Shogen K, Darzynkiewicz Z. (2008). *The cytotoxic ribonuclease Onconase targets RNA interference (siRNA)*. Cell Cycle. Oct;7(20):3258-61

29 Sorrentino S. (2010). *The eight human "canonical" ribonucleases: molecular diversity, catalytic properties, and special biological actions of the enzyme proteins*. FEBS Lett. Jun 3;584(11):2194-200

30 Gao, X. and Xu, Z. (2008) *Mechanisms of action of angiogenin*. Acta Biochim. Biophys. Sin. (Shanghai) 40, 619–624

31 Yang D, Rosenberg HF, Chen Q, Dyer KD, Kurosaka K, Oppenheim JJ. (2003). *Eosinophil-derived neurotoxin (EDN), an antimicrobial protein with chemotactic activities for dendritic cells*. Blood. Nov 1;102(9):3396-403

32 Deshpande RA and Shankar V. (2002). *Ribonucleases from T2 family*. Crit Rev Microbiol 28(2):79-122

33 Natalie Luhtala and Roy Parker. (2010). *T2 Family ribonucleases: ancient enzymes with diverse roles*. Trends Biochem. Sci. May;35(5):253-9

34 McClure BA and Franklin-Tong V. (2006). *Gametophytic self-incompatibility: understanding the cellular mechanism involved in 'self' pollen tube inhibition. Planta* 224(2): 233-45

35 Thompson, D.M. and Parker, R. (2009). *The RNase Rny1p cleaves tRNAs and promotes cell death during oxidative stress in Saccharomyces cerevisiae*. J. Cell. Biol. 185, 43–50

36 Roiz L, Smirnoff P, Bar-Eli M, Schwartz B, Shoseyov O. (2006). *ACTIBIND, an actin-binding fungal T2-RNase with antiangiogenic and anticarcinogenic characteristics*. Cancer 106, 2295–2308

37 Schwartz B, Shoseyov O, Melnikova VO, McCarty M, Leslie M, Roiz L, Smirnoff P, Hu GF, Lev D, Bar-Eli M.(2007). *ACTIBIND, a T2 RNase, competes with angiogenin and inhibits human melanoma growth, angiogenesis, and metastasis*. Cancer Res. 67, 5258–5266

38 Hauptschein R, Gamberi B, Pulivarthi R, Frigri F, Scotto L, et al. (1998). *Cloning and mapping of human chromosome 6q26–q27 deleted in B-cell non-Hodgkin lymphoma and multiple tumour types*. Genomics 50(2): 170-86

39 Taborelli M, Tibiletti MG, Martin V, Pozzi B, Bertoni F, Capella C. (2006). *Chromosome band 6q deletion pattern in malignant lymphomas*. Cancer Genet Cytogenet 165(2): 106-13

40 Tahara H, Smith A, Gas R, Cryns V, Arnold A. (1996). *Genomic localization of novel candidate tumour suppressor gene loci in human parathyroid adenomas*. Cancer Res 56(3): 599-605

41 Noviello C, Courjal F, Theillet C. (1996). *Loss of heterozygosity on the long arm of chromosome 6 in breast cancer: possibly four regions of deletion*. Clin Cancer Res 2(9): 1601-6

42 Yamada T, De Souza AT, Finkelstein S, Jirtle R. (1997). *Loss of the gene encoding mannose 6 phosphate/insulin-like growth factor II receptor is an early event in liver carcinogenesis*. Proc Natl Acad Sci USA 94(19): 10351-5

43 Hayashi Y, Raimondi S, Look T, Behm F, Kitchington G, Pui C, Rivera G, Williams D. (1990). *Abnormalities of the long arm of chromosome 6 in childhood acute lymphoblastic leukaemia*. Blood 76(8): 1626-30

44 Gaidano G, Hauptschein RS, Parsa NZ, Offit K, Rao PH, Lenoir G, Knowles DM, Chaganti RSK, Dalla-Favera R. (1992). *Deletions involving two distinct regions of 6q in B-cell non-Hodgkin lymphoma*. Blood 80: 1781-7

45 Colitti, Rodabaugh, Welch, Berkowitz, & Mok. (1998). *A novel 4 cM minimal deletion unit on chromosome 6q25.1-q25.2 associated with high grade invasive epithelial ovarian carcinomas*. Oncogene, 16; 555-559

46 Orphanos, McGown, Hey, Thorncroft, Santibanez-Koref, Russell, et al. (1995). *Allelic imbalance of chromosome 6q in ovarian tumours*. Br. J. Cancer 71, 666-669

47 Saito S, Saito H, Koi S, Sagae S, Kudo R, Saito J, Noda K, Nakamura Y. (1992). *Fine-scale deletion mapping of the distal long arm of chromosome 6 in 70 human ovarian cancers*. Cancer Res. 52, 5815-5817

48 Liu Y, Emilion G, Mungall AJ, Dunham I, Beck S, Le Meuth-Metzinger VG, Shelling AN, Charnock FM, Ganesan TS. (2002). *Physical and transcript map of the region between D6S264 and D6S149 on chromosome 6q27, the minimal region of allele loss in sporadic epithelial ovarian cancer*. Oncogene. Jan 17;21(3):387-99

49 Tibiletti MG, Trubia M, Ponti E, Sessa L, Acquati F, Furlan D, et al. (1998). *Physical map of the D6S149 D6S193 region on chromosome 6q27 and its involvement in benign surface epithelial ovarian tumours*. Oncogene 16, 1639-1642

50 Acquati F, Morelli C, Cinquetti R, Bianchi MG, Porrini D, Varesco L, Gismondi V, Rocchetti R, Talevi S, Possati L, Magnanini C, Tibiletti MG, Bernasconi B, Daidone MG, Shridhar V, Smith DI, Negrini M, Barbanti-Brodano G, Taramelli R. (2001). *Cloning and characterization of a senescence inducing and class II tumor suppressor gene in ovarian carcinoma at chromosome region 6q27*. Oncogene. Feb 22;20(8):980-8

51 Acquati F, Possati L, Ferrante L, Campomenosi P, Talevi S, Bardelli S, Margiotta C, Russo A, Bortoletto E, Rocchetti R, Calza R, Cinquetti R, Monti L, Salis S, Barbanti-Brodano G, Taramelli R. (2005). *Tumor and metastasis suppression by the human RNASET2 gene*. Int J Oncol. May;26(5):1159-68

52 Campomenosi P, Salis S, Lindqvist C, Mariani D, Nordstrom T, Acquati F, Taramelli R. (2006). *Characterization of RNASET2, the first human member of the Rh/T2/S family of glycoproteins*. Arch Biochem Biophys 449(1-2): 17-26

53 George P. Studzinski. (1999). *Cell growth, differentiation and senescence: a practical approach*. Oxford University Press

54 Lester BR, McCarthy JB. (1992). *Tumor cell adhesion to the extracellular matrix and signal transduction mechanisms implicated in tumor cell motility, invasion and metastasis*. Cancer Metastasis Rev. Mar;11(1):31-44

55 VanRooijen, and Sanders. (1994). *Liposome mediated depletion of macrophages: mechanism of action, preparation of liposomes and applications*. J. Immunol. Methods 174, 83-93

56 B. al-Sarireh B, Eremin O. (2000). *Tumour-associated macrophages (TAMS): disordered function, immune suppression and progressive tumour growth*. J R Coll Surg Edinb. Feb;45(1):1-16

57 Sica A, Larghi P, Mancino A, Rubino L, Porta C, Totaro MG, Rimoldi M, Biswas SK, Allavena P, Mantovani A. (2008). *Macrophage polarization in tumour progression*. Semin Cancer Biol. Oct;18(5):349-55

58 T.J. Shaw, M.K. Senterman, K. Dawson, C.A. Crane and B.C. Vanderhyden. (2004). *Characterization of intraperitoneal, orthotopic, and metastatic xenograft models of human ovarian cancer*. Mol Ther 10 (6), 1032–1042

59 Carpten J, Nupponen N, Isaacs S, Sood R, Robbins C et al. (2002). *Germline mutations in the ribonuclease L gene in families showing linkage with HPC1*. Nat Genet 30(2): 181-4

60 F.C. Noonan-Wheeler, W. Wu, K.A. Roehl, A. Klim, J. Haugen, B.K. Suarez, A.S. Kibel. (2006). *Association of hereditary prostate cancer gene polymorphic variants with sporadic aggressive prostate carcinoma*. Prostate 66; 49–56

61 Mosser DM, Edwards JP. (2008). *Exploring the full spectrum of macrophage activation*. Nat Rev Immunol. Dec;8(12):958-69.

62 Mantovani A, Sozzani S, Locati M, Allavena P, Sica A. (2002). *Macrophage polarization: tumor-associated macrophages as a paradigm for polarized M2 mononuclear phagocytes*. Trends Immunol. Nov;23(11):549-55

63 Mantovani A, Sica A. (2010). *Macrophages, innate immunity and cancer: balance, tolerance, and diversity*. Curr Opin Immunol. Apr;22(2):231-7

64 Rosenberg HF. (2008). *Eosinophil-derived neurotoxin / RNase 2: connecting the past, the present and the future*. Curr Pharm Biotechnol. Jun;9(3):135-40

65 Yang D, Chen Q, Su SB, Zhang P, Kurosaka K, Caspi RR, Michalek SM, Rosenberg HF, Zhang N, Oppenheim JJ. (2008). *Eosinophil-derived neurotoxin acts as an alarmin to activate the TLR2-MyD88 signal pathway in dendritic cells and enhances Th2 immune responses*. J Exp Med. Jan 21;205(1):79-90

66 Steinfelder S, Andersen JF, Cannons JL, Feng CG, Joshi M, Dwyer D, Caspar P, Schwartzberg PL, Sher A, Jankovic D. *The major component in schistosome eggs responsible for conditioning dendritic cells for Th2 polarization is a T2 ribonuclease (omega-1)*. J Exp Med. Aug 3;206(8):1681-90

67 Everts B, Perona-Wright G, Smits HH, Hokke CH, van der Ham AJ, Fitzsimmons CM, et al. (2009). *Omega-1, a glycoprotein secreted by Schistosoma mansoni eggs, drives Th2 responses*. J Exp Med. Aug 3;206(8):1673-8

68 Thompson DM, Parker R. (2009). *Stressing out over tRNA cleavage*. Cell. Jul 23;138(2):215-9.

69 Tang J, Hu M, Lee S, Roblin R. (2000). *A polymerase chain reaction based method for detecting Mycoplasma/Acholeplasma contaminants in cell culture*. J Microbiol Methods. Jan;39(2):121-6

70 Ventura A, Meissner A, Dillon CP, McManus M, Sharp PA, Van Parijs L, Jaenisch R, Jacks T. (2004). *Cre-lox-regulated conditional RNA interference from transgenes*. Proc Natl Acad Sci USA. Jul 13;101(28):10380-5